Palaeontology
The Palaeontological Association
www.palass.org

[Palaeontology, Vol. 56, Part 1, 2013, pp. 95–127]

TAXONOMIC REVISION OF *ISOCETUS DEPAUWI* (MAMMALIA, CETACEA, MYSTICETI) AND THE PHYLOGENETIC RELATIONSHIPS OF ARCHAIC 'CETOTHERE' MYSTICETES

by MICHELANGELO BISCONTI[1]*, OLIVIER LAMBERT[2,3] *and* MARK BOSSELAERS[3,4]

[1]Museo di Storia Naturale del Mediterraneo, via Roma 234, 57100 Livorno, Italia; e-mail: zoologia.museo@provincia.livorno.it
[2]Département Histoire de la Terre, Muséum National d'Histoire Naturelle, Rue Buffon 8, 75005 Paris, France
[3]Royal Belgian Institute of Natural Sciences, Rue Vautier 29, 1000 Brussels, Belgium
[4]Zeeland Royal Society of Sciences, Middelburg, The Netherlands
*Corresponding author.

Typescript received 8 June 2011; accepted in revised form 20 April 2012

Abstract: The taxonomic revision of *Isocetus depauwi* Van Beneden, 1880 was carried out through the description of a number of specimens assigned to this species by Van Beneden and Abel in the last decades of the 19th and the early decades of the 20th centuries. After detailed comparisons with the published record of archaic mysticetes, the genus and species are considered valid despite the incompleteness and poor preservation of the material. Diagnostic features are found in the morphology of the mandibular condyle, the angular process of the dentary and the thoracic vertebrae. The new species *Parietobalaena campiniana* is established based on a partial skeleton, including most of the skull and ear bones, previously assigned to *Isocetus depauwi* by Abel. *Parietobalaena campiniana* is described and compared in detail, and its phylogenetic relationships are assessed by a new large-scale cladistic analysis of 246 morphological characters scored for 46 taxa. The results support a basal position of the genus *Parietobalaena* in the radiation of Miocene 'cetotheres', the monophyly of Balaenoidea (Neobalaenidae and Balaenidae), Balaenopteroidea (Eschrichtiidae and Balaenopteridae), and Cetotheriidae and the paraphyly of 'cetotheres' *s.l.* The new superfamily Thalassotherii is established based on high bootstrap support and a number of morphological characters; Thalassotherii includes Balaenopteridae, Eschrichtiidae, Cetotheriidae and the basal 'cetothere' mysticetes with the exclusion of Balaenoidea, Eomysticetoidea and toothed mysticetes.

Key words: Belgium, Cetacea, Cetotheriidae, *Isocetus depauwi*, Miocene, Mysticeti, *Parietobalaena campiniana*, Thalassotherii.

In 1880, Van Beneden published the first description of *Isocetus depauwi* based on a few specimens from the area of Antwerp, Belgium, that, at that time, were not completely prepared. *Isocetus depauwi* is a small-sized baleen whale (Mammalia, Cetacea, Mysticeti) from the Miocene. Because of its bad preservation, Van Beneden was able to describe only part of a skull and listed few specimens that he assigned to the new genus. His diagnosis was limited to note that the 'apex of the skull' (whatever this means) was very delicate and that the anteroposterior exposition of the parietal at vertex was limited to 3 cm. He also assigned a dentary, seven cervical vertebrae, two thoracic vertebrae, two ribs and some unspecified limb bones to this genus.

In the fifth part of his *Description des ossements fossiles des environs d'Anvers*, Van Beneden (1886) gave a more detailed description of *Isocetus depauwi* and provided illustrations of the left dentary, a right tympanic bulla, seven cervical vertebrae, seven thoracic vertebrae, three lumbar vertebrae, a right ulna and a possible jugal bone. The skull mentioned in his earlier work was not illustrated with the exception of the possible jugal.

Abel (1938) assigned a new specimen to *Isocetus depauwi*. The new material was discovered in 1913 near Kessel, 17 Km ESE to Antwerp; Fig. 1). In his work, he illustrated the left dentary in lateral, dorsal and medial views, and a new skull in ventral view. At the time of Abel's publication, the dorsal side of the skull was still unprepared. He further noted that the skull mentioned by Van Beneden (1880, 1886) was lost. Further, comments on the vertebral morphology of *Isocetus depauwi* were published by Slijper (1936, p. 209).

doi: 10.1111/j.1475-4983.2012.01168.x

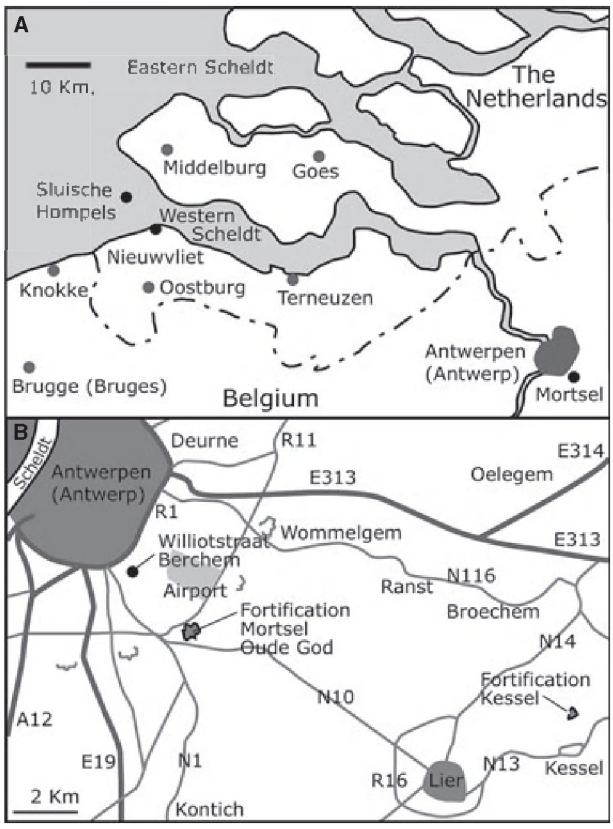

FIG. 1. Geographic maps showing the localities of discovery of the specimens described in the present paper. A, northern Belgium and southern Holland showing the geographic position of Antwerp. B, main localities cited in the text.

Other students assigned mysticete fossils to *Isocetus* based on the descriptions of Van Beneden and Abel. In fact, Zbyszewski (1953) reported a mandible of *Isocetus depauwi* from the Helvetian of Portugal, also Roth (1978) mentioned the presence of *Isocetus depauwi* from the Gram Formation of Denmark, and Morgan (1994) cited the presence of ?*Isocetus* sp. in the Agricola Fauna, Bone Valley Formation, Florida. The fragmentary nature of the type materials, however, suggests caution when assigning specimens to this taxon whose affinities are still unclear. Even so, McKenna and Bell (1997) placed *Isocetus* in the family Cetotheriidae. At the time they were publishing their book, there were different interpretations of Cetotheriidae, which, in the previous decades, had acquired the status of a sort of taxonomic basket where all the mysticetes lacking synapomorphies of living families were included (Fordyce and Barnes 1994).

In the last few years, a consensus about the status of this family was reached. Based on the studies of Bouetel and de Muizon (2006) and Whitmore and Barnes (2008), the family is now well diagnosed and includes mysticete genera displaying a long ascending process of the maxilla with anteriorly diverging lateral border that interdigitates with the frontal. Phylogenetic analyses of the Mysticeti provided by Bouetel and de Muizon (2006), Bisconti (2007*a*, 2008) and Steeman (2007, 2009) supported the monophyly of a small group of mysticetes with this character (and others) that are now considered to form the *core* of Cetotheriidae *s.s.*; these are *Cetotherium rathkii* Brandt (1873), *Metopocetus durinasus* Cope (1896), *Herpetocetus transatlanticus* Whitmore and Barnes (2008), *Nannocetus eremus* Kellogg (1929) and *Piscobalaena nana* Pilleri and Siber (1989).

All the other archaic mysticetes previously assigned to Cetotheriidae *s.l.* ('cetotheres') that lack the synapomorphy described above are excluded from Cetotheriidae *s.s.* For this reason, Whitmore and Barnes (2008), in their taxonomic revision, included the 'cetotheres' in Cetotheriidae *incertae sedis* (including also *Isocetus*) implying that 'cetotheres' and Cetotheriidae form a monophyletic group. Uhen *et al.* (2008) included *Isocetus* in Mysticeti *incertae sedis*, paralleling the proposal of Steeman (2010) who suggested that the status of *Isocetus* and *Isocetus depauwi* will be pending until the type material is reviewed.

In the last few years, new evidence has come to light based on the complete preparation (realized by M. Boss.) of the skull described in part by Abel (1938). By means of this newly available material, the ear bones of this specimen could be studied for the first time. For this reason, we decided to start a revision of the type material of *Isocetus depauwi* through new morphological descriptions, comparisons and phylogenetic analysis, in a way to understand the taxonomic status of the taxon and to investigate the phylogenetic relationships of the archaic 'cetothere' mysticetes. These studies result in the recognition of a new, large-scale superfamily-rank clade of mysticetes, which includes Balaenopteridae, Eschrichtiidae, Cetotheriidae *s.l.* and *s.s.*, but excludes Balaenidae, Neobalaenidae, Eomysticetoidea and toothed mysticetes (Fig. 2). We call this clade Thalassotherii; we provide a diagnosis and a definition of it and discuss its importance in taxonomic and evolutionary terms.

Institutional abbreviations. AMNH, American Museum of Natural History, New York, United States of America; RBINS, Royal Belgian Institute of Natural Sciences, Brussels, Belgium; USNM, National Museum of Natural History, Smithsonian Institution, Washington D.C., United States of America.

MATERIAL

We examined the following specimens:

1. RBINS M.396-R.370: a partial skeleton including a moderately well-preserved proximal part of the left dentary and distal part of the right dentary, a fragment of the left tympanic bulla, the right ulna,

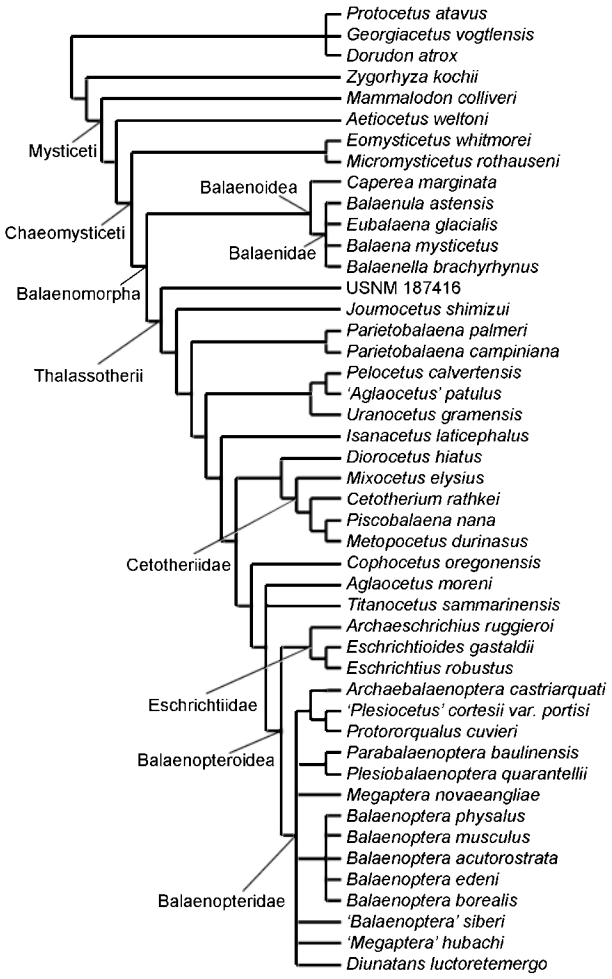

FIG. 2. Phylogenetic relationships of baleen-bearing mysticetes as determined by the cladistic analysis performed in the present paper. Strict consensus of 246 trees. Tree length, 912 steps; consistency index, 0.3849; consistency index excluding uninformative characters, 0.3760; rescaled consistency index, 0.2746; homoplasy index, 0.6151; retention index, 0.7135.

a fragment of the atlas, the axis, third-to-seventh cervical vertebrae, seven thoracic vertebrae, eight lumbar vertebrae and several highly fragmented ribs. According to the RBINS catalogue, this is the first specimen that has been figured by Van Beneden (1886). The specimen was found during the building of a fortification (Fort 4) in Oude God ('Vieux-Dieu' in French), a locality in Mortsel (Antwerp suburbs, Belgium), in 1867.

2. RBINS M.399-R.4018: a skull and part of the left dentary, atlas, third-to-seventh cervical vertebrae, two thoracic vertebrae and two hyoid fragments (one of them is lost). The specimen was found at the fort of Kessel (ESE to Antwerp, Belgium) in January 1913, and was described and figured by Abel (1938).
3. RBINS M.397-R.1525: an isolated right tympanic bulla found in Fort 4 (Oude God, Mortsel, Belgium), in 1867.
4. RBINS M.398-R.1526: an isolated posterior thoracic vertebra found in Fort 4 (Oude God, Mortsel, Belgium), in 1867.
5. RBINS R.1553: fragment of dentary, found in the area of Antwerp.
6. RBINS R.1554: isolated lumbar vertebra, found in the area of Antwerp.
7. RBINS R.1556: isolated axis, found in the area of Antwerp.
8. RBINS R.1557: isolated atlas, found in the area of Antwerp.
9. RBINS R.1566: isolated right scapula, found in the area of Antwerp.
10. RBINS R.1615: fragment of skull vertex, fragment of atlas, distal fragment of right premaxilla and anterior apex of the left dentary, found in the area of Antwerp.
11. RBINS R.279: skull fragment with exoccipitals, occipital condyles, foramen magnum and part of the basioccipital, found in the area of Antwerp.
12. RBINS R.357: isolated caudal vertebra, found in the area of Antwerp.
13. RBINS R.920: five lumbar vertebrae, found in the area of Antwerp.
14. Nonnumbered: one thoracic, two lumbar and two caudal vertebrae, found in the area of Antwerp.

Our analysis revealed that these specimens, previously assigned to *Isocetus depauwi*, are too fragmentary to be safely assigned to whatever mysticete taxon. For this reason, we consider them Mysticeti indet. Descriptions and interpretations of these specimens are fully provided in the Supporting Information published in the website of *Palaeontology*.

The following specimens were recently discovered and prepared by one of us (M. Boss.) and are included here because they are strictly related to the subject of this paper:

1. RBINS M.2010: isolated right periotic originating from Sluische Hompels (Western Scheldt estuary in front of Nieuwvliet, Cadzand, The Netherlands, in dredged sands), in 2009.
2. RBINS M. 2011: isolated left squamosal found in the Williotstraat (Berchem, Antwerp, Belgium), in 2010.

These specimens are fully described in the Supporting Information published in the website of *Palaeontology*. In the same Supporting Information are also provided the measurements of the specimens examined in the present paper (Tables S1–S8).

Anatomical terminology follows Miller (1923), Kellogg (1928, 1965, 1968*a*), Nickel *et al.* (1991), Fordyce (1994), Schaller (1999) and Mead and Fordyce (2010).

SYSTEMATIC PALAEONTOLOGY

Class MAMMALIA Linnaeus, 1758
Order CETACEA Brisson, 1762
Suborder MYSTICETI Flower, 1864
Parvorder BALAENOMORPHA Geisler and Sanders, 2003

Superfamily THALASSOTHERII superfam. nov.

Derivation of name. *Thalassos*, Greek, sea; *Therii*, Latin, mammal beasts. The name recalls the title of a historical monograph on fossil cetaceans written by an important Italian palaeontologist (Portis 1885). Adjective: thalassotherian(s).

Diagnosis. In the following text, character transformations diagnostic for Thalassotherii new superfamily that are used in the cladistic analysis of the present paper are put between brackets (character numbers refer to the character list presented as Supporting Information). Diagnostic features: short longitudinal exposure of interorbital region of the frontal because parietal superimposes on it (character 58: 2 → 3); moderate transverse constriction of supraoccipital (character 108: – → 0) (the symbol – means that the character is absent or, in other words, not developed); lateral borders of supraoccipital concave anterior to the transverse constriction (character 109: – → 0); endocranial opening of facial canal separated from the internal acoustic meatus by the interposition of a thick crista transversa (character 129: 0 → 1); presence of postcoronoid crest and fossa in dentary (character 179: 0 → 1); postcoronoid crest and fossa well developed (character 180: – → 0); mandibular condyle oriented posteriorly (character 188: 1 → 2).

Discussion. It will be shown in this paper that Thalassotherii is a clade established on a number of synapomorphies and that its recognition helps into making order in the phylogeny and taxonomy of baleen-bearing mysticetes. Thalassotherii is to be intended as a superfamily-rank clade including several families of living and extinct mysticetes (Balaenopteridae, Cetotheriidae, Eschrichtiidae and additional stem-thalassotherian mysticetes). By the establishment of Thalassotherii as a new superfamily, the rank of Balaenopteroidea has to be changed into epi family. Thus, the parvorder Balaenomorpha includes three superfamilies: Eomysticetoidea, Balaenoidea and Thalassotherii; Balaenoidea includes two families (Balaenidae and Neobalaenidae), and Thalassotherii includes three families at least (see above).

In the last decade, several phylogenetic analyses have resulted in the recognition of a large clade including Cetotheriidae *s.s.*, Cetotheriidae *s.l.*, Eschrichtiidae and Balaenopteridae to the exclusion of Balaenidae, Neobalaenidae, Eomysticetoidea and toothed mysticetes (Kimura and Ozawa 2002; Bisconti 2005, 2007*a*, *b*, 2008, 2010; Steeman 2007, 2009; Kimura and Hasegawa 2010; Marx 2011). However, this large clade has never been named, and ambiguous terms have been used to identify the taxa that belong to it, but that lack the synapomorphies of identified families (e.g. Geisler and Luo's (1996) archaic mysticetes, Uhen *et al.*'s (2008) Cetotheriidae *s.l.* and Fordyce and de Muizon's (2001) 'cetotheres'). Thalassotherii is defined by a number of morphological characters related to the periotic, supraoccipital and dentary. Most of the species hypothetically assigned to Thalassotherii share the diagnostic traits listed in the diagnosis. Two exceptions are noteworthy: (1) the lateral border of the supraoccipital is different from the shared state in *Pelocetus*, '*Aglaocetus*' *patulus*, *Uranocetus* and *Isanacetus*; (2) the crista transversa within the internal acoustic meatus is very thin making the endocranial opening of the facial canal very close to the depression including the tractus spiralis foraminosus and the foramen singulare in *Pelocetus*, '*Aglaocetus*' *patulus*, *Uranocetus*, *Isanacetus* and extant *Balaenoptera* and *Megaptera* species. We suggest that the morphology of *Pelocetus*, '*A.*' *patulus*, *Uranocetus* and *Isanacetus* is the result of a seconday loss of the derived states in both the supraoccipital and the periotic. We speculate that *Pelocetus*, '*A.*' *patulus* and *Uranocetus* should belong to a new thalassotherian family, but we feel that more morphological support is necessary to establish it. As far as *Balaenoptera* and *Megaptera* are concerned, it should be noted that the diagnostic morphology of Thalassotherii is observed during postnatal growth and in some adult individuals of *Balaenoptera physalus* (Bisconti 2001; Bisconti and Bosselaers in prep.), thus confirming the assignment made here. In the genus *Balaenoptera*, the postcoronoid crest and fossa are present but vestigial (Bisconti 2010).

Definition. Thalassotherii includes Cetotheriidae *s.l.*, Cetotheriidae *s.s.*, Eschrichtiidae and Balaenopteridae. In phylogenetic terms (Sereno 1998, 1999), Thalassotherii is defined as USNM 187416, *Balaenoptera*, their last common ancestor and all the descendants of this ancestor. Phylogenetically, the most basal named taxon of Thalassotherii is *Joumocetus shimizui* Kimura and Hasegawa, 2010. The establishment of Thalassotherii in the taxonomy of mysticetes makes the term Cetotheriidae *s.l.* obsolete because the latter and Cetotheriidae *s.s.* do not form a monophyletic group. Cetotheriidae *s.l.* is to be changed into basal thalassotherians or thalassotherian stem group or Thalassotherii *sedis mutabilis*.

Stratigraphic distribution. Based on the cladogram of Figure 2, we estimate the origin of Thalassotherii to be latest Oligocene in age because earliest offshoots of the other Balaenomorpha are from Late Oligocene – Early Miocene. In particular, the earliest Balaenidae are documented from the earliest Miocene of Argentina (Bisconti 2003) (but see Fordyce 2002 for the discovery of a late Oligocene balaenid from the New Zealand). Thalassotherians

include the living members of the genera *Balaenoptera*, *Megaptera* and *Eschrichtius*.

Geographic distribution. Thalassotherii includes several genera (i.e. *Isanacetus, Diorocetus, Pelocetus, Cetotherium, Aglaocetus, Mixocetus, Parietobalaena, Joumocetus, Titanocetus, Cophocetus, Archaebalaenoptera, Plesiobalaenoptera, Parabalaenoptera, Protororqualus, Balaenoptera, Megaptera*) whose geographic distributions can be assessed through the geographic dataset available by Paleobiology Database (Uhen 2010). Based upon this dataset, the geographic distribution of Thalassotherii encompasses all the world oceans.

Family INCERTAE SEDIS

Genus ISOCETUS Van Beneden, 1880

Type species. *Isocetus depauwi* Van Beneden, 1880, only included species.

Diagnosis. As for *Isocetus depauwi*, only included species.

Isocetus depauwi Van Beneden, 1880
Figures 4–12

Holotype. Van Beneden did not designate a holotype for this species. He figured several specimens assigned to *I. depawi* that are now known as type material (Fig. 3). According to the point 73.3 of the Article 73 of the online version of the International Code of Zoological Nomenclature (available at http://www.nhm.ac.uk/hosted-sites/iczn/code/), these are syntypes. Among them, the partial skeleton RBINS M.396-R.370 is the first figured specimen and shows sufficient diagnostic features to be used as lectotype.

Lectotype. Partial skeleton RBINS M.396-R.370, by present designation.

Horizon and locality. Berchem Formation, Antwerp Sands Member, late Early to Middle Miocene (*c.*16.5–15.2 Ma) according to Louwye et al. (2000) and Louwye (2005). The specimen was found in Oude God (at the time, the locality was cited in French as 'Vieux-Dieu'), in the town of Mortsel, south-east suburbs of Antwerp, during the building of a fortification (Fort 4), in 1867 (Fig. 1). The geographic coordinates of the discovery site are as follows: N 51°10′23″; E 04°27′39″. The associated fauna includes eurhinodelphinids, *Squalodon*, physeteroids and other cetaceans (e.g. Lambert 2005, 2008).

Emended diagnosis. Angular process of the dentary located more anteriorly than the posterior articular surface of the condyle; angular process dorsoventrally short; groove for the internal pterygoid muscle located only along the medial side of the dentary; mandibular condyle round and transversely wide; distinctive concavity posterior to the metapophysis in the anterior thoracic vertebrae.

Discussion. According to Abel (1938), the original skull of *Isocetus depauwi* was lost decades prior to 1938. Therefore, it is not possible to check the presence of the specific characteristics that Van Beneden (1880) suggested were diagnostic for this taxon, namely (1) apex of the skull very delicate and (2) dorsal exposure of the parietal limited to 3 cm. Nevertheless, it is difficult to understand what Van Beneden meant when he stated that the skull of *I. depauwi* has a very delicate apex. In our opinion, this character cannot be accepted as a diagnostic feature in the absence of further specifications. The dorsal exposure of the parietal is a character observed in all the archaic mysticetes, being a primitive mammalian condition (Carroll 1988). In particular, the extension of the dorsal exposure of the parietal is longer in Oligocene baleen-bearing Eomysticetoidea (Sanders and Barnes 2002*a*, *b*) and shorter in the subsequent radiation of thalassotherian

FIG. 3. Reproduction of Van Beneden's (1886) plate 73 representing cervical and thoracic vertebrae of specimen RBINS M.396-R.370 (lectotype of *Isocetus depauwi*). Upper row from left to right: seven cervical vertebrae and seven thoracic vertebrae in left lateral view. Lower row from left to right: atlas in anterior and posterior views, axis in anterior and posterior views, and the following three cervical vertebrae in anterior views. Not to scale.

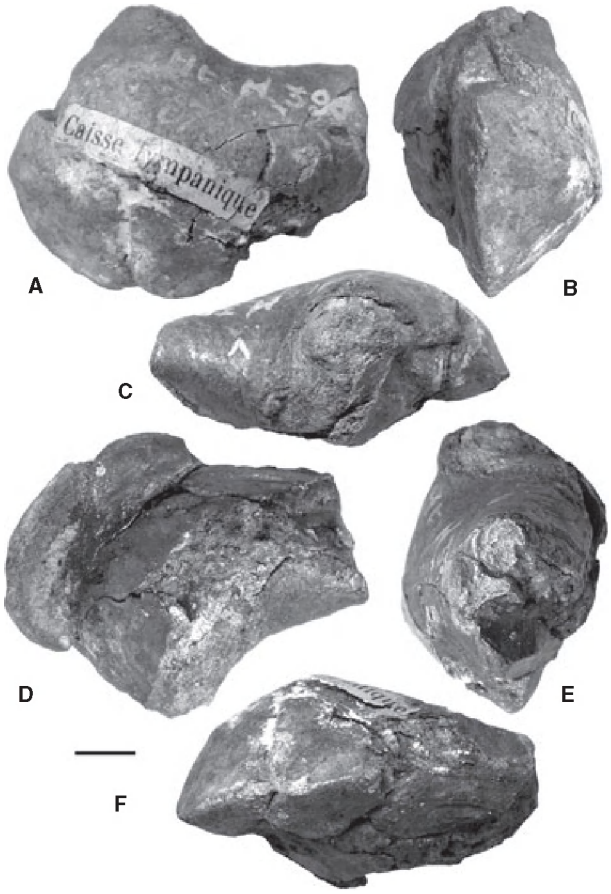

FIG. 4. Tympanic bulla of the lectotype of *Isocetus depauwi* (RBINS M.396-R. 370). A, medial view; B, posterior view; C, dorsal view; D, lateral view; E, anterior view; F, ventral view. Scale bar represents 10 mm.

mysticetes. In balaenids, the parietal is superimposed by the supraoccipital; for this reason, it is not exposed between the supraoccipital and the posterior border of the frontal (Bisconti 2003). There is not consensus about the denomination of this skull part: here we call it cranial vertex (or vertex) because it involves the same osteological features that occur at the cranial vertex of odontocetes according to Mead and Fordyce (2009). In balaenopterids, the parietal may be either exposed as a subtle stripe of bone which is only a few mm in length, as in *Balaenoptera physalus* Linnaeus (1758), or not exposed as in *Balaenoptera siberi* Pilleri (1989) and *B. musculus* Linnaeus (1758). In Cetotheriidae and Eschrichtiidae, the exposure of the parietal at the vertex is much reduced and the parietals meet along the longitudinal axis of the skull forming a short and laterally concave relief (Bisconti 2008). The length of the exposure of the parietal at the cranial vertex can be of taxonomic interest if incorporated into a proportional ratio, but its absolute value should be regarded with caution. In fact, such a length might depend on the ontogenetic age of the specimen or on its overall size. For instance, in the basal thalassotherian *Parietobalaena palmeri* Kellogg (1924), the exposure of the parietal at vertex ranges from *c.* 20 to *c.* 40 mm based on the ontogenetic age of the specimens (Kellogg 1924, 1968*d*). For this reason, it appears inappropriate to base a diagnosis of a mysticete genus on such a character.

In the holotype of *Isocetus depauwi*, only one diagnostic character of Thalassotherii is preserved: the posterior orientation of the mandibular condyle. Moreover, the tympanic bulla of the holotype of *I. depauwi* exhibits characters that allow to infer its placement in a radiation subsequent to the origin of Balaenomorpha and to exclude it from Balaenidae and Neobalaenidae. The posterior cleft (*sensu* Luo and Gingerich, 1999, p. 44) of the tympanic bulla disappears in all Balaenomorpha; in Balaenidae and Neobalaenidae, the tympanic cavity is low and the bulla is roughly squared in ventral view. In basal thalassotherians and Eomysticetoidea, the bulla is approximately pear-shaped in ventral view. The lack of the posterior cleft and the pear-like shape of the bulla and, more importantly, the morphology of the mandibular condyle allow assigning *Isocetus depauwi* to Thalassotherii. Additional skeletal material is needed to make more precise assessments.

Description

Tympanic bulla. Only a small portion of the left tympanic bulla of the holotype is preserved (Fig. 4). It includes part of the involucrum, which is slightly rounded and bears a rather robust emergence of the posterior pedicle. The dorsal bulge, located posteriorly on the involucrum, is weak. The dorsomedial border digradates anteriorly. This fragmentary bulla is 41 mm long, and its maximum width is 25 mm (Table S1).

Dentary. The partial left dentary shows a slight external curvature and a high dorsoventral curvature (Fig. 5). In transverse section, the medial surface is anteriorly convex but becomes flat-to-slightly concave approaching the coronoid process. The lateral surface of the dentary is highly transversely convex. The dorsal surface of the dentary is almost totally worn. The ventral border has a sharp and acute edge (Fig. 6). On the medial surface, the mylohyoidal groove is absent and the mandibular foramen is broken. Only the base of the coronoid process is preserved. The mandibular condyle faces posteriorly and shows a wide surface, which is dorsoventrally and transversely convex. The condyle is transversely wide, projects laterally and has a concave lateral surface. The angular process is well separated from the condyle by a notch-shaped pterygoid groove that is well developed medially. The angular process is well developed and protrudes ventrally. It is oriented medially, with the condyle being located much more laterally. Measurements are provided in Table S2.

The fragment of right dentary is rather straight and bears one mental foramen (Fig. 7). The surface is almost completely worn.

FIG. 5. Left dentary of the lectotype of *Isocetus depauwi* (RBINS M.396-R.370). A lateral view. B, dorsal view. C, medial view. Scale bar represents 100 mm.

The anterior end is dorsoventrally expanded, but transversely narrow. Measurements are in Table S2.

Vertebrae. The vertebral epiphyses are not fused with the bodies, suggesting that this partial skeleton belongs to a juvenile or subadult individual. The axial skeleton includes seven cervical vertebrae (C1–C7) (Figs 8 and 9), seven thoracic vertebrae (T1–T7), four lumbar vertebrae (possibly L4–L6 and L8) and one indeterminate vertebra. Measurements are provided in Table S3.

The atlas (C1) is only partially preserved, with the whole right dorsolateral corner being absent. The transverse process is short and stocky. The dorsolateral corner is very high. The outline of the neural canal is squared.

The axis (C2) has a short, stocky and flat ventral transverse process with a triangular lateral apex. The neural canal is oval-shaped and is 55 mm wide and 40 mm high (see other measurements in Table S3). The neural process is short and rounded. The anterior articular facet is convex but largely eroded; the posterior articular surface is concave. The vertebral epyphysis is heart-shaped.

The body of C3 is delicate and small. The dorsal and ventral borders of the body are parallel; the neural canal is wide (59 mm in width). Dorsal and ventral emergences of the transverse processes are preserved.

The body of C4 is anteroposteriorly narrow, but it appears wider in anterior view than C3. It bears a sharp ventral keel. The body has an oval outline in anterior view. The emergences of the transverse processes are present. The neural canal is about 72 mm in width.

In C5 the dorsal border of the body is straight. The ventral surface bears a sharp keel. The transverse processes are delicate, small and flat. The neural arch bears anterior metapophyses that are flat and located rather laterally. The width of the neural arch is 64 mm, and the height (as it can be reconstructed) is 33 mm.

The ventral surface of the body of C6 is rounded. The ventral transverse process is not present. The metapophyses are located distally on the sides of the neural arch and are posteriorly bounded by distinctive concavities. C7 is almost completely destroyed.

The body of T1 is oval in anterior view (Fig. 10). The metapophyses are located distally on the sides of the neural arc and are posteriorly bounded by concavities. The transverse process is flat, short and stocky, and bears an articular facet for a single-headed rib. The neural arch is 79 mm wide and 40 mm (as preserved) high.

The body of T2 is short. The transverse processes are wide and flat. The transverse diameter of the neural channel is 67 mm. The neural arch is missing.

In T3 the neural arch is low and wide (30 mm high; 66 mm wide). Wide metapophyses are located on the sides of the neural arc; metapophyses are slightly oblique and descending externally. The transverse process is almost cylindrical, bearing only one articular facet for the head of the rib. The ventral surface of the body displays a rounded keel.

T4 has similar characters as T3, but its transverse processes are broken, and the neural process is longer than that of T3. The width of the neural arc is 64 mm, and the height is 34 mm. A postzygapophysis is located on the emergence of the transverse process.

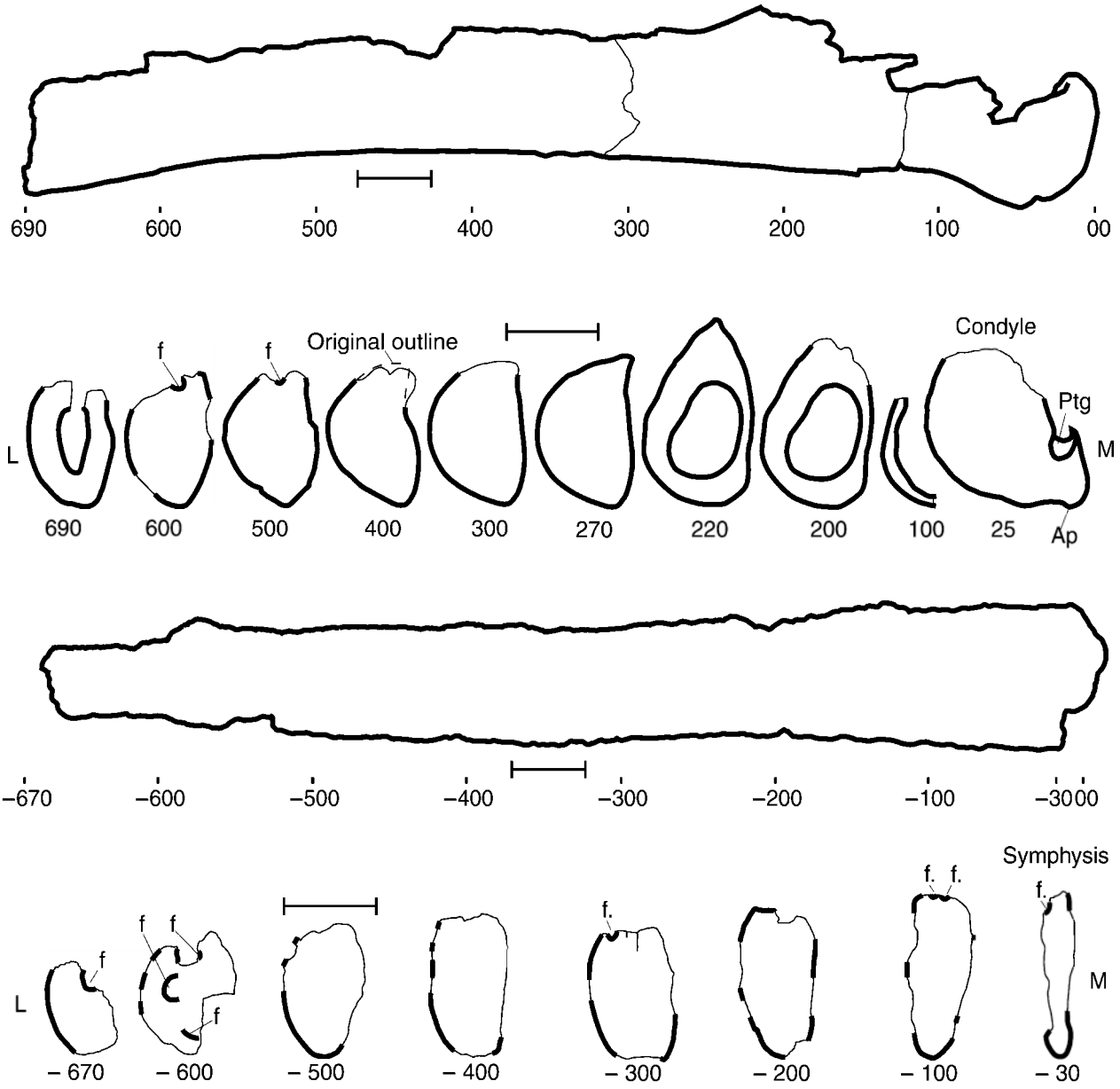

FIG. 6. Transverse sections of left and right dentaries of the lectotype of *Isocetus depauwi* (RBINS R.396-M.370). A, schematic representation of left dentary. B, transverse sections of left dentary. C, schematic representation of right dentary. D, transverse sections of right dentary. Posterior portions are on the left side of the figure in A and B and on the right side of the figure in C and D. Thick lines represent the actual profiles of the bones; thin lines represent reconstructed parts. Numbers represent the distance (in mm) from the posterior end of the relative dentary. Abbreviations: ap, angular process; f, mandibular foramen; L, lateral; M, medial; ptg, pterygoid groove. Scale bars represent 100 mm.

The body of T5 is longer than that of T3, and its ventral surface shows a rounded keel. The width of the neural arc is 53 mm, and the height is 33 mm. The transverse processes are flat, short and stocky with articular facet for the head of the rib. The metapophyses are slightly transversely extended. A wide and flat postzygapophysis is located on the emergence of the transverse process.

The body of T6 shows a round ventral keel. The transverse processes are short and stocky, and bear an articular facet for a single-headed rib. The metapophyses show an articular facet located laterally. The neural arch is well preserved and is surmounted by a high neural process. The width of the neural arc is 47 mm, and the height is 35 mm.

The body of L4 is damaged, but a sharp ventral keel is preserved; only the emergence of the transverse processes is preserved, showing that the processes were flat. The emergence is located at the middle of the lateral surface. The arch is lost.

FIG. 7. Right dentary of the lectotype of *Isocetus depauwi* (RBINS M.396-R. 370). A, lateral view. B, dorsal view. C, medial view. Scale bar represents 100 mm.

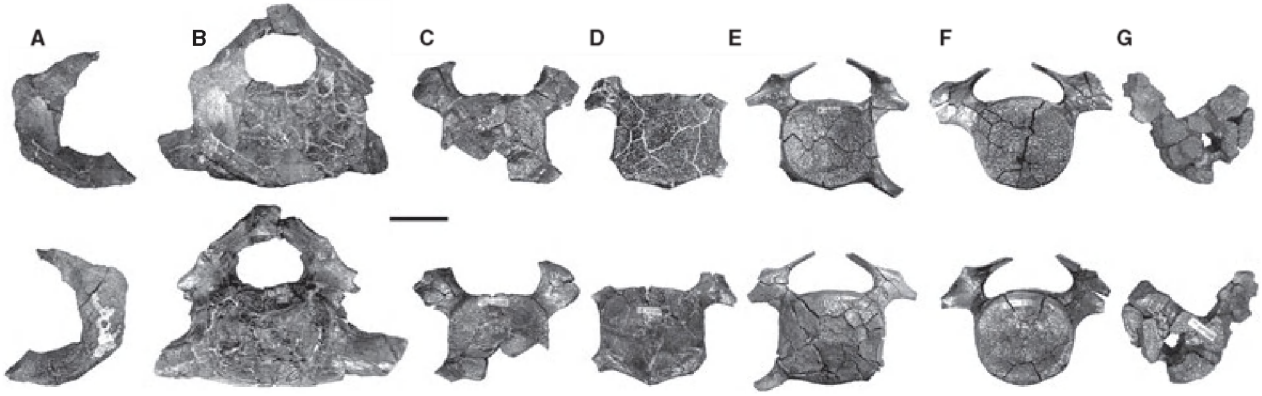

FIG. 8. Cervical vertebrae of the lectotype of *Isocetus depauwi* (RBINS M.396-R.370). Upper row: anterior view; lower row: posterior view. A, atlas. B, axis. C–G, 3rd-to-7th cervical vertebrae. Scale bar represents 50 mm.

The lateral sides of L5 are damaged; the transverse processes emerge at a similar position as in L4. In anterior view, the outline of the epyphysis is oval-shaped.

In L6 the epyphyses are not preserved; the vertebra is fragmentary and eroded; only part of the body is preserved.

The ventral keel of L8 is sharp; the lateral sides of the body are highly concave. Parts of long and flat transverse processes emerge from the middle of the sides. The neural arch is not preserved. In anterior view, the outline of the epyphysis is oval-shaped.

Ribs. Only a fragment of the first rib is sufficiently well preserved to be anatomically informative (Fig. 11). The capitulum is missing. The ventral part is badly damaged owing to pyrite decomposition. The corpus is broadly semicircular and strongly flattened anteroposteriorly. A few small remnants of other fragmentary and badly damaged ribs are preserved.

Ulna. The proximal portion of the right ulna is preserved (Fig. 12). The length of the body is 226 mm. The diaphysis is narrow (41 mm in minimum diameter) and anteriorly convex. The olecranon process is squared and is 87 mm in posterior height. The anteroposterior diameter of the proximal end is 116 mm. The proximal epiphysis is missing. The articular surface is 45 mm in anteroposterior diameter and 39 mm in transverse diameter.

Comparison

The partial skeleton RBINS M.396-R.370 lacks most of the anatomical parts usually employed for comparative purposes. The tympanic bulla is extremely fragmentary. It is not possible to know whether it had an anterolateral

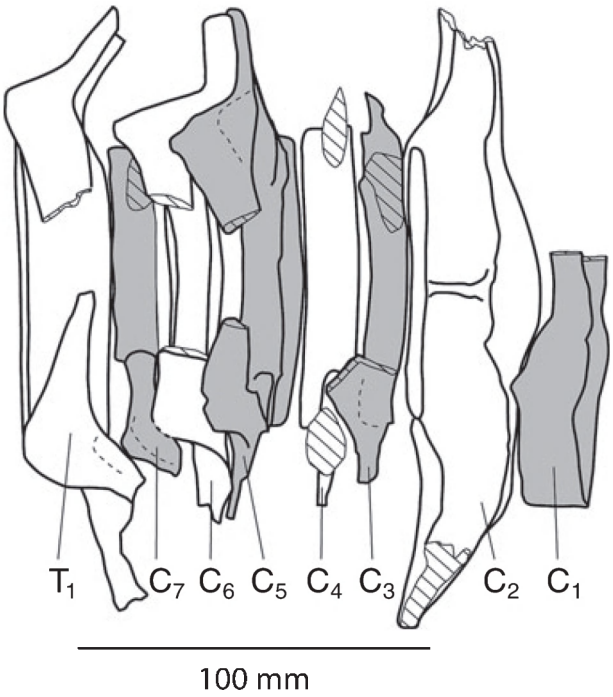

FIG. 9. Cervical vertebrae of the lectotype of *Isocetus depauwi* (RBINS M.396-R. 370) in dorsal view. C1–C7 = atlas-to-7th cervical vertebrae; T1 = 1st thoracic vertebra.

FIG. 11. Rib (possibly the first) of the lectotype of *Isocetus depauwi* (RBINS M.396-R.370) in anterior view. Scale bar represents 100 mm.

expansion or not, and whether its opening for the Eustachian tube was high or low. For these reasons, it cannot help in the determination of the taxonomy and relationships of the specimen.

The proximal fragment of the dentary bears a pterygoid groove on its medial surface. It separates the articular surface of the condyle from the angular process. Other archaic mysticetes have the pterygoid groove in a similar position, among them: *Parietobalaena palmeri* (Kellogg 1968*d*), *Parietobalaena* sp. (Kimura *et al.* 1998), *Thinoc-*

FIG. 10. First-to-seventh thoracic vertebrae of the lectotype of *Isocetus depauwi* (RBINS M.396-R.370) in right lateral view. Anterior is on the right side. Scale bar represents 100 mm.

FIG. 12. Lectotype of *Isocetus depauwi* (RBINS M.396-R.370): proximal end and diaphysis of ulna. Scale bar represents 100 mm.

etus arthritus Kellogg (1969) and *Diorocetus hiatus* Kellogg (1968*b*). This character is also observed in several specimens held by the RBINS and previously figured by Van Beneden (1886, pls 2, 5, 14, 19, 70).

The angular process of the dentary is located rather anteriorly and protrudes ventrally. Such a condition is observed in an indeterminate thalassotherian from Japan (Kimura 2002) although in that specimen the angular process has a more irregular shape.

The mandibular condyle appears much more rounded in posterior view in all the other archaic mysticetes (*sensu* Geisler and Luo 1996) and can be considered exclusive of this animal, representing a diagnostic feature of the genus. In *Pelocetus calvertensis* Kellogg (1965), the mandibular condyle is rather round and wide; the angular process is located anterior to the mandibular condyle and protrudes ventrally. However, the groove for the internal pterygoid muscle crosses the posterior face of the dentary and can be observed in lateral view. Moreover, in this taxon, the angular process is much smaller than the condyle as far as the dorsoventral diameter of the condyle is concerned, but it is also much more transversely expanded.

The presence of a distinctive concavity posterior to the metapophysis in the thoracic vertebrae is not observed in other mysticetes and is exclusive to *Isocetus depauwi*. In other mysticetes, the neural arch is smooth posterior to the metapophysis. This trait is considered diagnostic of the genus.

The specimen M.399-R.4018 was assigned to *Isocetus depauwi* by Abel (1938), although it was not completely prepared. The dentary of M.399-R.4018 is rather different from that of the lectotype of *Isocetus depauwi*: the condyle is markedly smaller and is transversely narrow and appears dorsoventrally elongated (Fig. 13). Moreover, the angular process of the dentary M.399-R.4018 is dorsoventrally longer than that of *Isocetus depauwi*. These differences support the inclusion of the specimen M.399-R.4018 in a different taxon (see below).

Discussion

The lectotype skeleton of *Isocetus depauwi* is largely fragmentary. The lack of most of the anatomical parts usually employed for comparisons and phylogenetic inference makes it difficult to assess its taxonomic and phylogenetic affinities. The presence of some peculiar traits allows the formal diagnosis of the taxon, but the only suggestion of phylogenetic affinity is given by the position of the groove for the internal pterygoid muscle in the posteromedial side of the dentary. As stated above, such a groove occurs in the same position only in *Diorocetus hiatus*, *Parietobalaena palmeri*, *Parietobalaena* sp. and *Thinocetus arthritus*, as well as in a series of specimens figured by Van Beneden (1886). The taxonomy of these Van Beneden specimens is currently under debate, as many of them became *nomina dubia* or *nomina nuda* in a revision by Steeman (2010), based on ear bones only. A new and thorough study of this material (most of which is now incertae sedis), including other skeletal elements, should be undertaken to clarify the taxonomy of these specimens and to base the systematic assignments on more extensive mor-

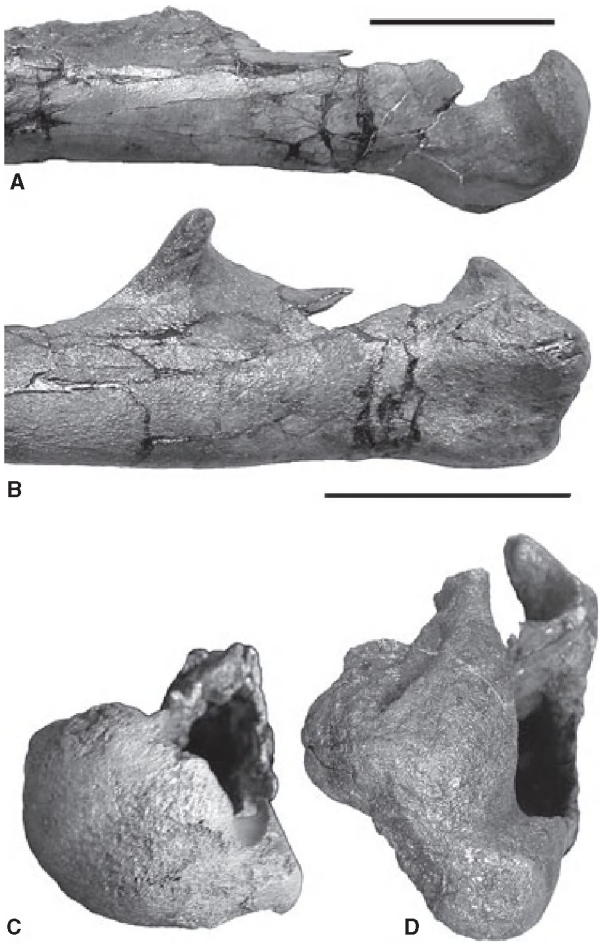

FIG. 13. Comparison between posterior portions of left dentary of the lectotype of *Isocetus depauwi* and the holotype of *Parietobalaena campiniana*. A, posterior part of the left dentary of *Isocetus depauwi* in lateral view. B, posterior part of left dentary of *Parietobalaena campiniana* in lateral view. C, posterior part of left dentary of *Isocetus depauwi* in posterior view. D, posterior part of left dentary of *Isocetus depauwi* in posterior view. Scale bar represents 100 mm.

phological evidence. In *Diorocetus hiatus*, the angular process is anteroposteriorly short and bears a round ventral surface; the angular process protrudes slightly posteriorly to the articular surface of the mandibular condyle. In *Parietobalaena palmeri*, the angular process is strongly reduced anteroposteriorly and protrudes ventrally. Moreover, in *P. palmeri*, the angular process is slightly posterior to the articular surface of the condyle, in contrast to the condition in *Isocetus depauwi*, in which the angular process is slightly anterior to the articular surface of the mandibular condyle.

In both *Parietobalaena palmeri* and *Diorocetus hiatus*, the angular process protrudes slightly posteriorly, resembling Cetotheriidae *s.s.* (Kellogg 1968*b*, *d*; Whitmore and Barnes 2008).

The proportions of the articular surface of the mandibular condyle and of the angular process of *Pelocetus calvertensis* resemble the morphology observed in *Isocetus depauwi*, but the different development of the groove for the internal pterygoid muscle and the stronger angular process observed in *Pelocetus* support different taxonomic assignments.

The peculiar morphology observed in the thoracic vertebrae of *Isocetus depauwi* resembles the morphological condition seen in the anterior thoracic vertebrae of *Eschrichtius robustus* Lilljeborg, 1861. Close inspection of the skeleton AMNH 34260 previously assigned to *Eschrichtius gibbosus* Erxleben (1777) revealed that the metapophysis of T1–T9 is located distally with respect to the neural arch and that a concave facet is located between the metapophysis and the neural arch. The distal location of the metapophyses resembles the vertebral morphology of *Isocetus depauwi*, but, in this species, a concave facet is located posteriorly to the metapophysis, not medially.

In the specimen M.399-R.4018, assigned to *I. depauwi* by Abel (1938), the mandibular condyle is much narrower transversely (Fig. 13); the angular process is located ventrally under the articular surface of the condyle and is more rounded ventrally and more developed transversely. In posterior view, the dentary of the specimen RBINS M.399-R.4018 is substantially compressed transversely, in contrast to the dentary of *Isocetus depauwi* that is more transversely expanded. In the two thoracic vertebrae associated with the partial skeleton RBINS M.399-R.4018, the metapophyses are only partially preserved; the metapophysis of T5 is located laterally of RBINS M.399-R.4018, in a position similar to that of the metapophyses of *Isocetus depauwi*. However, the presence of a posterior concavity cannot be unambiguously confirmed.

Based on the differences observed in the dentary, we assign the specimen RBINS M.399-R.4018 to a different taxon, *Parietobalaena campiniana* new species, the description of which is provided below.

In conclusion, the fragmentary skeleton RBINS M.396-R.370 represents a mysticete species with peculiar characters in the dentary and in the vertebral column. These characters allow its recognition and separate it from other, well diagnosed mysticete taxa. In this sense, the species *Isocetus depauwi* is retained independent from the bad preservation of its remains. In fact, these remains are not sufficient to be used in a cladistic analysis but are sufficient to warrant a reliable diagnosis that will be of great help in the recognition of other *Isocetus* finds elsewhere.

The morphology of *Isocetus* dentary is highly characteristic owing to the strong ventral protrusion of the angular process, suggesting highly active masseter and pterygoid muscles during feeding. The function of the wide mandibular condyle is still difficult to interpret.

Genus PARIETOBALAENA Kellogg, 1924

Type species. Parietobalaena palmeri Kellogg, 1924.

Emended diagnosis of genus. A basal thalassotherian with very short-to-absent ascending process of the maxilla, very short lateral process of the maxilla (*sensu* Barnes and McLeod 1984, p. 2), anterior end of nasal located anterior to the anterior border of the supraorbital process of the frontal, presence of a concavity in the lateral side of the squamosal, endocranial opening of facial canal separated from the foramen including the tractus spiralis foraminosus and the foramen singulare by a wide crista transversa, dorsal surface of periotic strongly protruded dorsally to form a convex dome, short anterior process of the periotic, anterior process of periotic abruptly depressed anteriorly to the central portion of the dorsal surface of the periotic (the dorsally convex dome).

Discussion. The following text reproduces the emended diagnosis that Kellogg (1968*d*, p. 176) published to replace the first diagnosis published by Kellogg (1924, pp. 1, 2) (numbers are ours): (1) parietals meet medially to form a ridge between the apex of the supraoccipital shield and the frontals; (2) maxillary, premaxillary and nasal sutural contact grooves extended backward on frontals beyond level of preorbital angle of supraorbital process; (3) rostrum tapering towards extremity; (4) transverse temporal crest developed on supraorbital process of frontal on mature skulls; (5) nasals located for most part anterior to level of preorbital angle of supraorbital processes; (6) zygomatic process of squamosal slender, attenuated anteriorly and extended forward to or almost to elongated postorbital projection of supraorbital process of frontal; (7) postglenoid process directed more downward than backward, flattened on its posterior face and rounded distally; (8) occipital condyles small; (9) exoccipitals directed obliquely downward and backward, with lateral end projecting backward beyond level of articular surface of condyle on adult skulls; (10) pars cochlearis of periotic with strongly convex dome or apex extended ventrally; (11) a short narrow fossa of variable depth behind rim of fossa for stapedial muscle and above fenestra rotunda and its projecting shelf extends across posterior face of pars labyrinthica to its cerebral face. Tympanic bulla and periotic resemble in some details those of *'Idiocetus' laxatus* Van Beneden (1886, pl. 54, figs 3–4); (12) a deep groove for attachment of internal pterygoid muscle present below articular surface of condyle and above angle on internal surface of posterior end of mandible.

After many decades of study, some of Kellogg's characters are to be questioned in the light of new observations of individual variation. In particular, characters (1), (2), (3), (4), (5), (6) and (12) are observed in several basal thalassotherians, including *Diorocetus hiatus, Pelocetus calvertensis, Isanacetus laticephalus* Kimura and Ozawa (2002), and *'Aglaocetus' patulus* Kellogg (1968*c*), so it cannot be considered diagnostic at the genus level. Character (7) is observed in *Megaptera novaeangliae* Brisson (1762), *Diunatans luctoretemergo* Bosselaers and Post (2010), and *P. calvertensis*. Character (8) appears too general to be useful for a diagnosis. Character (9) is observed in *'A.' patulus*, *P. calvertensis*, *D. hiatus*. Character (10) is observed also in *P. calvertensis*, *I. laticephalus* and *'A.' patulus*. A strongly convex dome is also present in *Balaena mysticetus* Linnaeus (1758) and in archaeocetes such as *Zygorhiza kochii* Reichenbach in Carus (1847) and *Dorudon atrox* Andrews (1906); it should therefore be considered a primitive character of baleen-bearing mysticetes. However, in *Parietobalaena*, this character is particularly evident because of the strong reduction in the anterior process, which is highly depressed from the dorsal surface of the central portion of the periotic (the periotic dome). Similar to *Parietobalaena* are the periotics of *Heterocetus affinis* Van Beneden and Gervais (1868) (RBINS M.605a-R.301) and *Idiocetus laxatus* Van Beneden (1880) (RBINS M.727-R.61) assigned, respectively, to *Parietobalaena affinis* and *P. laxata* by Steeman (2010), based on ear bone morphology. The periotic M.605a-R.301 (elected by Steeman (2010) to be the lectotype of *Parietobalaena affinis* together with the tympanic bulla M.605b-R.301) lacks the anterior process and shows a stronger convex dome with uniformly concave suprameatal fossa; the tympanic bulla differs from that of *Parietobalaena palmeri* because its posterior border is perpendicular to the long axis of the bulla rather than oblique and because the posteromedial part of the bulla is convex rather than being concave as in the holotype of *P. palmeri*. The periotic M.727-R.61 (elected by Steeman (2010) to be the lectotype of *Parietobalaena laxata*) shows a longer anterior process, a more triangular dome in medial view, a much longer posterior process and a clearly concave posterodorsal portion of the suprameatal area. In these respects, the periotic M.727-R.61 is clearly different from that of *Parietobalaena palmeri*. These observations suggest that additional work is necessary to support the inclusion of this material within *Parietobalaena*. Given that the morphological support of Steeman's (2010) revision appears scanty, we provisionally consider *Heterocetus affinis* and *Idiocetus laxatus* as valid taxa pending a revision of all the referred skeletal material.

Parietobalaena campiniana sp. nov.
Figures 14–28

Derivation of name. The specific name *campiniana* derives from the name of a region located in the NE of Flanders (Belgium)

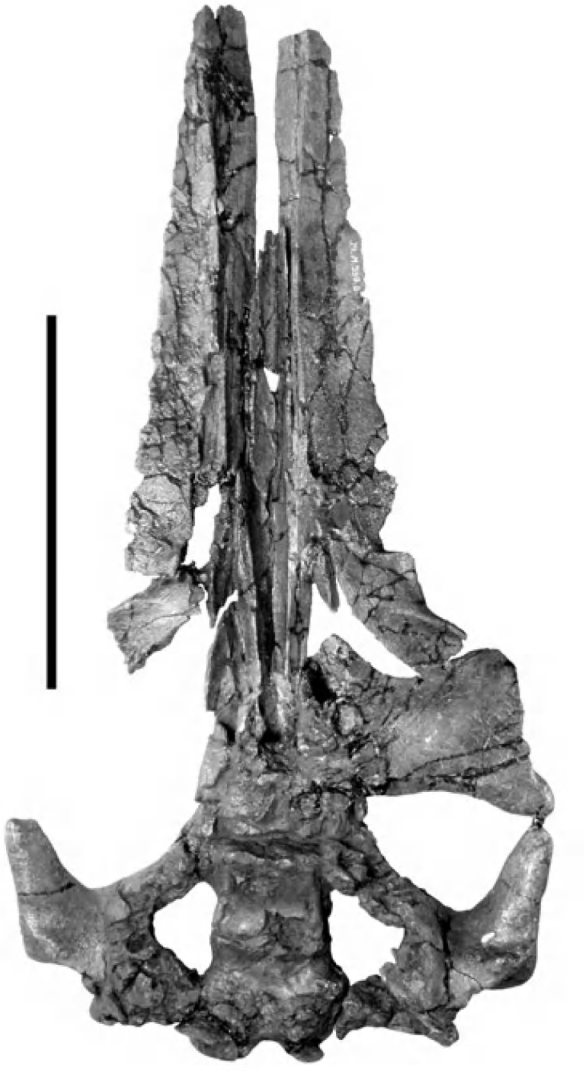

FIG. 14. Holotype skull of *Parietobalaena campiniana* (RBINS M.399-R.4018) in dorsal view. Scale bar represents 300 mm.

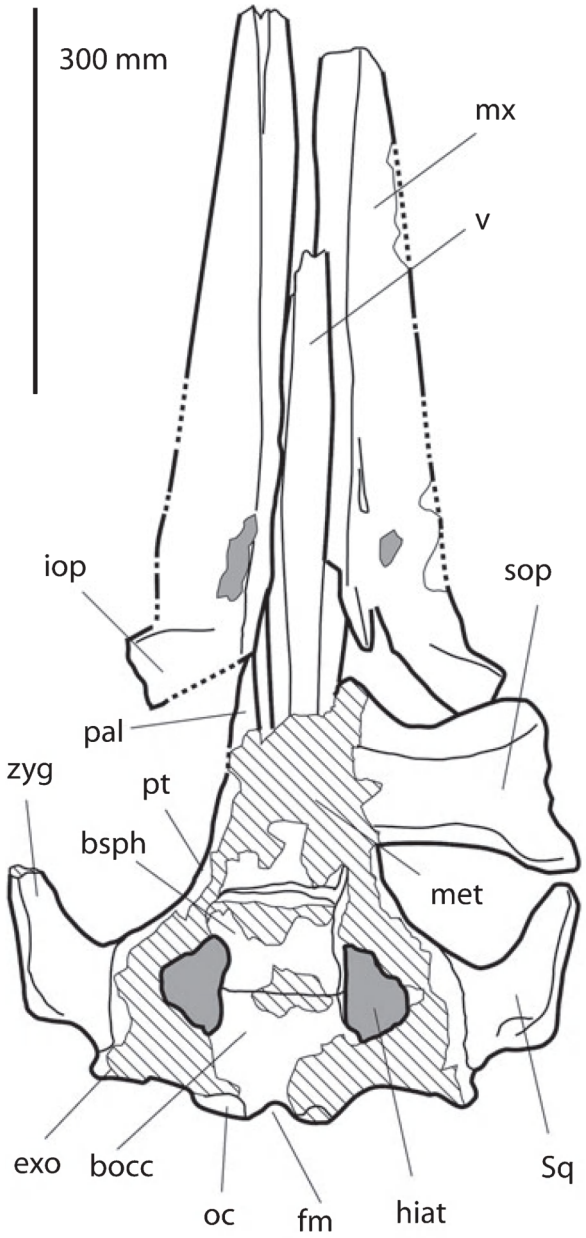

FIG. 15. Schematic representation of the holotype skull of *Parietobalaena campiniana* (RBINS M.399-R.4018) in dorsal view. Thick lines represent actual bone profiles; broken lines are missing parts; grey areas represent foramina. Scale bar represents 300 mm. Anatomical abbreviations: bocc, basioccipital; bsph, basisphenoid; exo, exoccipital; fm, foramen magnum; hiat, hiatus cranicus; iop, infraorbital process; met, mesethmoid; mx, maxilla; oc, occipital condyles; pal, palatine; pt, pterygoid; sop, supraorbital process of the frontal; sq, squamosal; v, vomer; zyg, zygomatic process of the squamosal.

and SE of the Netherlands called De Kempen (in Dutch), La Campine (in French) and campina (in Latin). The village and the Fort of Kessel, where the holotype specimen was found, are located in the south-eastern part of this region.

Holotype. RBINS M.399-R.4018 (Fig. 14); a skull and part of the left dentary, atlas, third-to-seventh cervical vertebrae, two thoracic vertebrae and one hyoid fragment. Some parts of the specimen were described and figured by Abel (1938).

Horizon and locality. The specimen was found in the Fort of Kessel (geographic coordinates of the site: N 51°09′02″; E 04°37′40″) in January 1913 (Fig. 1). A sample of sediment associated with the specimen was analysed by Lambert and Louwye (2006) for microfossils, especially dinoflagellates, to assess the chronostratigraphic age of this and other specimens from the same level. The analysis revealed that the specimen is dated from the Middle Miocene, tentatively late Langhian to early Serravallian, between c.15 and 13.2 Ma (Lambert and Louwye 2006).

Referred specimens. RBINS M.2010, an isolated periotic collected from reworked Miocene sands at the beach of the Scheldt estu-

FIG. 16. Skull of the holotype of *Parietobalaena campiniana* (RBINS M.399-R.4018) in ventral view. Thick lines represent actual bone profiles; broken lines are missing parts; grey areas represent foramina. Scale bar represents 300 mm.

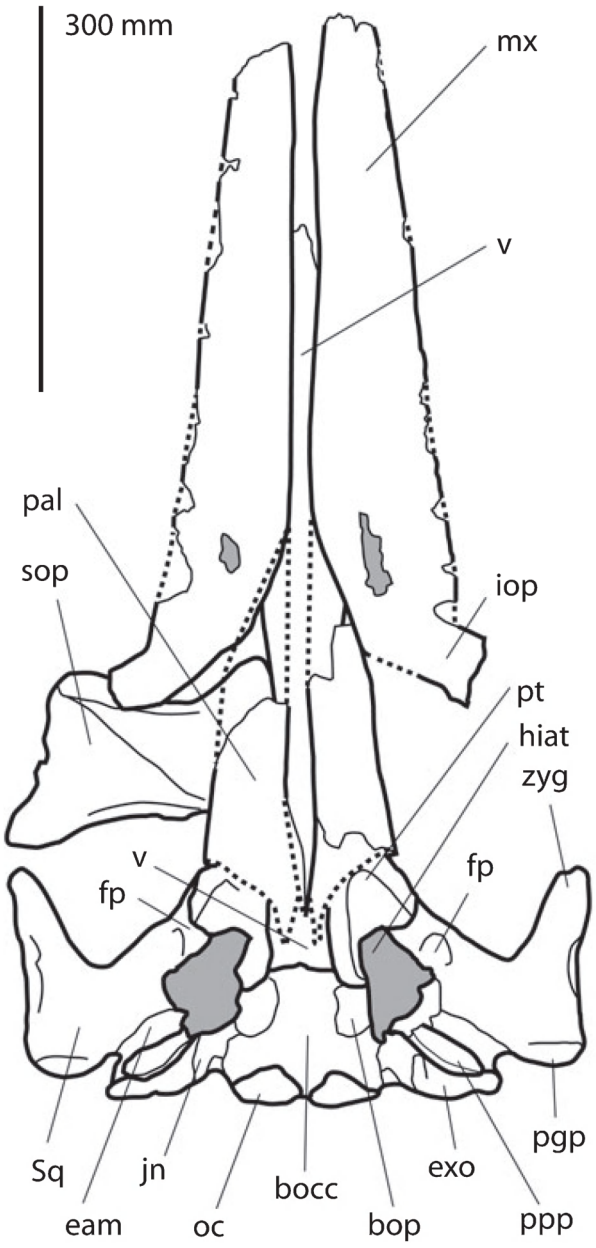

FIG. 17. Schematic representation of the skull of the holotype of *Parietobalaena campiniana* (RBINS M.399-R.4018) in ventral view. Scale bar represents 300 mm. Anatomical abbreviations: bocc, basioccipital; bop, basioccipital descending process; eam, external acoustic meatus; exo, exoccipital; fp, foramen pseudo-ovale; mx, maxilla; hiat, hiatus cranicus; iop, infraorbital process of the frontal; jn, jugular notch; oc, occipital condyle; pal, palatine; pgp, postglenoid process of squamosal; ppp, posterior process of periotic; pt, pterygoid; sq, squamosal; v, vomer; zyg, zygomatic process of the squamosal.

ary in Nieuwvliet, near Cadzand, originating from Sluissche Hompels (N 51°26′05″; E 03°25′02″) in the Western Scheldt estuary, The Netherlands (Riemslag 1998). RBINS M.2011, an isolated squamosal found in Berchem (Belgium), at a construction site in the Williotstraat (N 51°11′10″; E 04°26′09″); the specimen was found *in situ* in the Antwerp Sands Member, *Turritella eryna* horizon (late Burdigalian – early Langhian), of the Berchem Formation; the age of the specimen can be constrained from 16.7 to 15.1 Ma according to Louwye *et al.* (2010).

Diagnosis of species. Parietobalaena campiniana shares with *P. palmeri* several synapomorphies of the genus *Parietobalaena*: short lateral process of the maxilla, presence of a dorsal protrusion in the central portion of the periotic (periotic dome), anterior process of the periotic abruptly depressed from the periotic dome. As a species of *Parietobalaena*, it differs from *P. palmeri* in lacking the ventral protrusion of the angular process of the dentary, in having a stronger and shorter postorbital corner of the

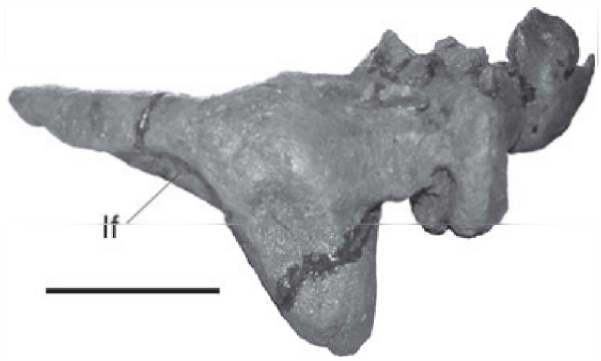

FIG. 18. Left squamosal of the holotype of *Parietobalaena campiniana* (RBINS M.399-R.4018), in lateral view showing the lateral fossa (lf). Anterior is on the left side. Scale bar represents 100 mm.

supraorbital process of the frontal and in having a longer and stronger supraorbital process of the frontal as a whole.

Description

General. The skull is fragmentary; only the basicranium, the squamosals and parts of the frontal, maxilla, vomer and dentary are preserved. The two periotics and tympanic bullae have been detached from the skull and prepared for study. Measurements are provided in the Supporting Information published online in the website of *Palaeontology*.

Premaxilla. Missing.

Maxilla. Like most of the skull, the maxilla is largely fragmentary. The lateral border is preserved on the right side, only in the posterior portion of the bone and in a few fragments located more anteriorly. It is elevated relative to the dorsolateral surface of the maxilla. The lateral process of the maxilla is some 4 cm long and tapers towards its apex. It is posteriorly fused with the infraorbital plate, which is preserved only in part and superimposed dorsally by the supraorbital process of the frontal. The medial border of the maxilla is raised above the lateral surface at the level of the narial fossa.

Judging from the length of the lateral process of the maxilla and from the orientation of the posterior-most border of the maxilla, the lateral edge of the maxilla was mainly elongated along the midline in dorsal view and the rostrum was narrow at the base (anterior to the emergence of the lateral process of the maxilla).

Even if the premaxilla is entirely missing, in baleen-bearing mysticetes, the premaxilla is lodged in an elongated cavity included between the maxillae along the midline of the skull (Figs 14 and 15). The lateral border of this cavity is parallel to the lateral border of the premaxilla. In the skull M399/R. 4018, the lateral edge of the cavity that holds the premaxilla is well preserved from the narial fossa to the anterior end of the rostrum (as preserved), indicating that the lateral border of the premaxilla was straight anterior to the narial fossa.

It is not possible to assess the total length of the rostrum because the anterior ends of the premaxilla and of the maxilla are missing. Moreover, it is impossible to describe the posteromedial corner of the maxilla because that part is missing. The dorsal surface of the maxilla is so damaged that it is impossible to assess the total number of the maxillary foramina unambiguously.

In ventral view, the medial border of the maxilla forms a ventral convexity holding the vomer (Figs 16 and 17). This convexity has a transversely rounded surface. In the ventral surface of the maxilla, a series of longitudinally oriented grooves for the vasculature of the baleen are located close to the ventromedial convexity, and a series of grooves oriented laterally and anteriorly are located more laterally.

Vomer. Part of the vomer is preserved under the narial fossa. The posterodorsal end of the vomer is attached to the presphenoid, forming two ascending laminae; the ethmoid was probably originally wedged between them, but it is lost. The vomer is strongly concave with a rounded dorsal surface. In ventral view, its posterior end is covered by the palatines for most of its extension. The vomerine crest projects posteriorly along the longitudinal axis of the skull and separates the choanae. The plate of the vomer from which the vomerine crest projects terminates slightly posteriorly to the anteromedial corner of the hiatus cranicus.

Palatine. Both palatines are preserved (Figs 16 and 17). The anterior border is oriented obliquely to the longitudinal axis of the skull, with its anteromedial corner being located more anteriorly than the posterolateral corner. The posterior border is substantially parallel to the anterior border. Measurements are reported in Table S4.

Frontal. Only the right supraorbital process of the frontal is preserved (Figs 14 and 15). It is rather broad and has a slightly convex dorsal surface. The temporal ascending crest is nearly absent being reduced and rounded. It is visible only near the postorbital corner. The orbit is low, long and uniformly rounded. The preorbital process is laterally short and rounded. The postorbital corner protrudes much more laterally than the preorbital corner. The anterior border of the supraorbital process of the frontal is remarkably concave in its medial half (viewed dorsally); the posterior border is slightly concave and forms a concavity medial and posterior to the narrow and protruding postorbital corner.

Most of the ventral surface of the supraorbital process of the frontal is occupied by an anteroposteriorly concave surface, which extends laterally (Figs 16 and 17). The anterior border of this surface is sharply edged and bears an anterior notch a few centimetre medial to the orbit.

Nasal, lacrimal, jugal, parietal, interparietal. Missing.

Squamosal. The anterior-most portion and the mediodorsal part of the squamosal are not preserved. The zygomatic process of the squamosal is elongated and transversely narrow; its anterior end is narrow and rounded. The dorsal edge of the zygomatic process of the squamosal is transversely rounded. In lateral view, the dorsal edge of the zygomatic process is straight and horizon-

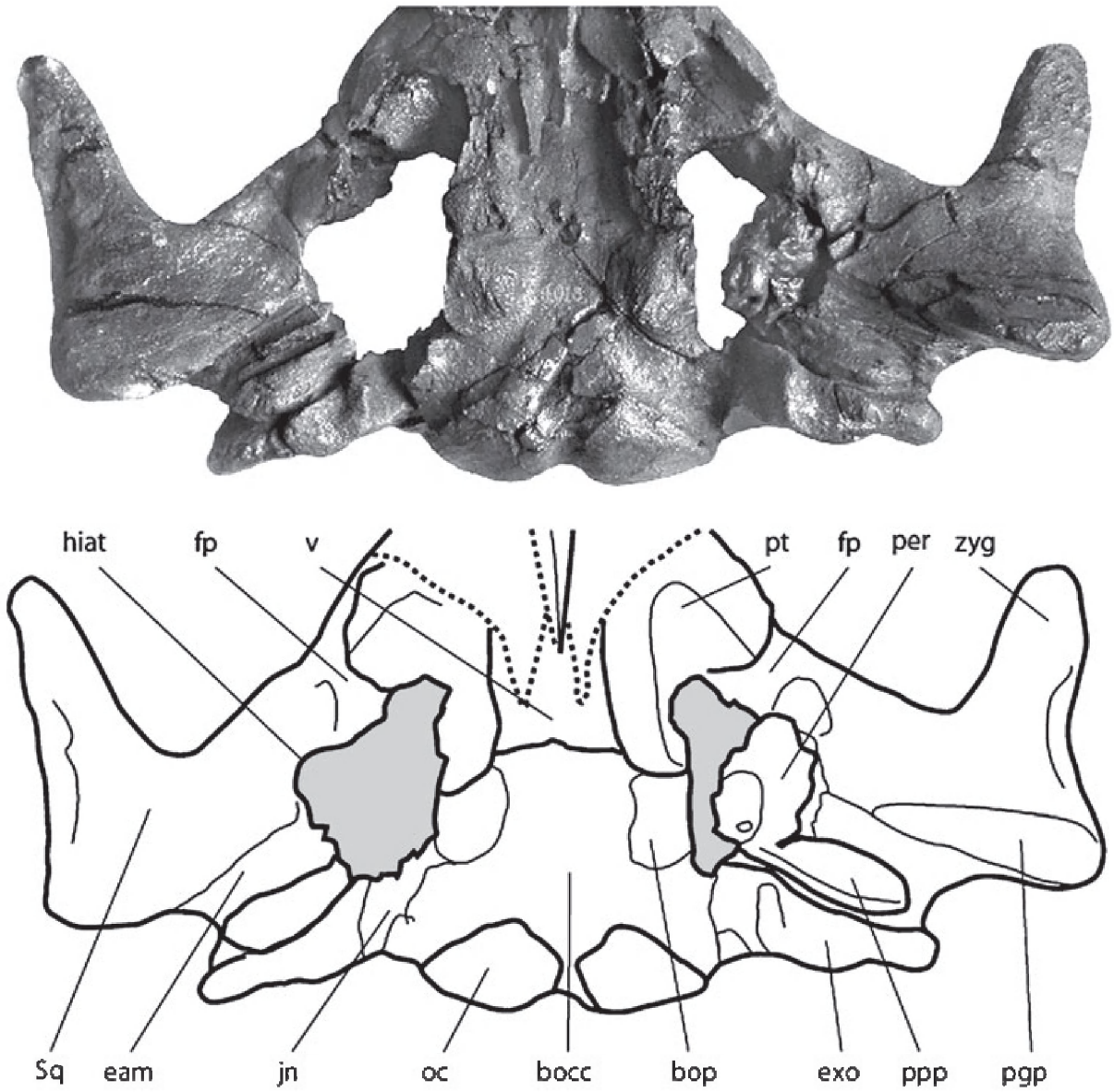

FIG. 19. Basicranium of the holotype of *Parietobalaena campiniana* (RBINS M.399-R.4018) in ventral view (left side) with left periotic still in articulation. A, photograph plate. B, schematic representation. Not to scale. Anatomical abbreviations: aped, anterior pedicle for attach with tympanic bulla; boc, basioccipital; bop, basioccipital descending process; eam, external acoustic meatus; exo, exoccipital; fp, foramen pseudo-ovale; fpo, falciform process of squamosal; hiat, hiatus cranicus; jn, jugular notch; oc, occipitaal condyle; pal, palatine; pgp, postglenoid process of squamosal; ppp, posterior process of periotic; prom, promontorium; pt, pterygoid; ptf, pterygoid fossa; sq, squamosal; v, vomer.

tal (Fig. 18). The secondary squamosal fossa is absent. The lateral surface of the zygomatic process of the squamosal is only slightly divergent from the longitudinal axis of the skull. In lateral view, the ventral border of the zygomatic process of the squamosal forms a wide concavity corresponding to the glenoid fossa of the squamosal. On both sides of the skull, laterally to the zygomatic process of the squamosal, there is an additional concavity located on the lateral surface of the squamosal (Fig. 18). We term it *lateral zygomatic concavity* (new term).

The postglenoid process is located more ventrally than the ventral surface of the zygomatic process of the squamosal and is elongated transversely. The glenoid fossa of the squamosal is, thus, wider posteriorly. The postglenoid process is thick dorsally; it is oriented slightly ventrally and posteriorly (the posterior wall is inclined about 5 degrees with respect to the vertical plane). Distally and medially it tapers forming a sharp medioventral crest.

The lateral squamosal crest is located above the postglenoid process. It is thin, blade-like and distinctly everted, overhanging the sternomastoid fossa posteriorly. Medially and dorsally, the crest is broken. Therefore, it is not clear whether it is continuous and whether it was in contact with the lambdoid crest. The sternomastoid crest is deep, medially and laterally long, more

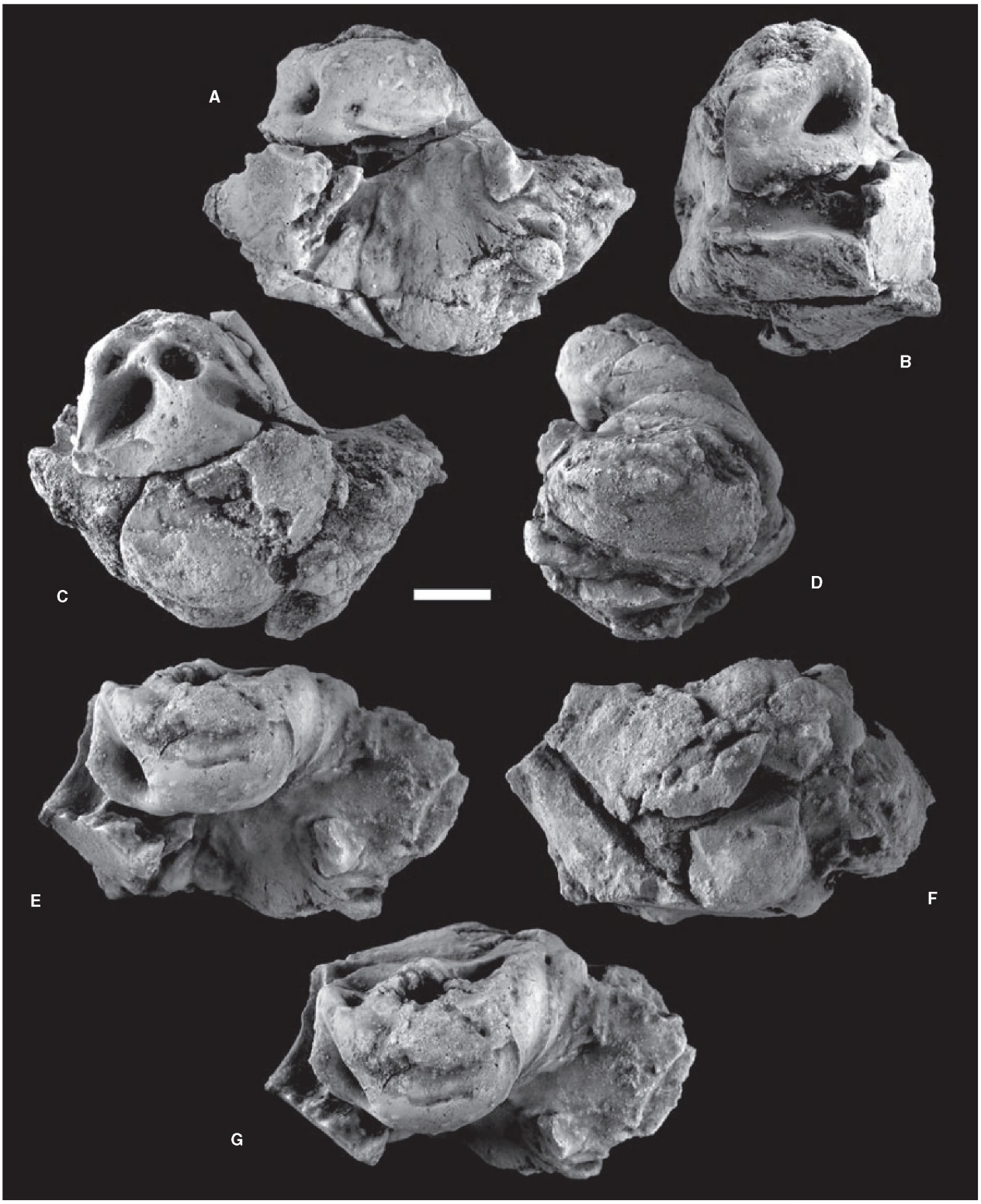

FIG. 20. Right periotic of the holotype of *Parietobalaena campiniana* (RBINS M.399-R.4018) without posterior process. A, posterolateral view. B, lateral view. C, posterior view. D, ventral view. E, medial view. F, posteromedial view. G, dorsal view. H, anterior view. Scale bar represents 10 mm. Specimen coated with ammonium chloryde.

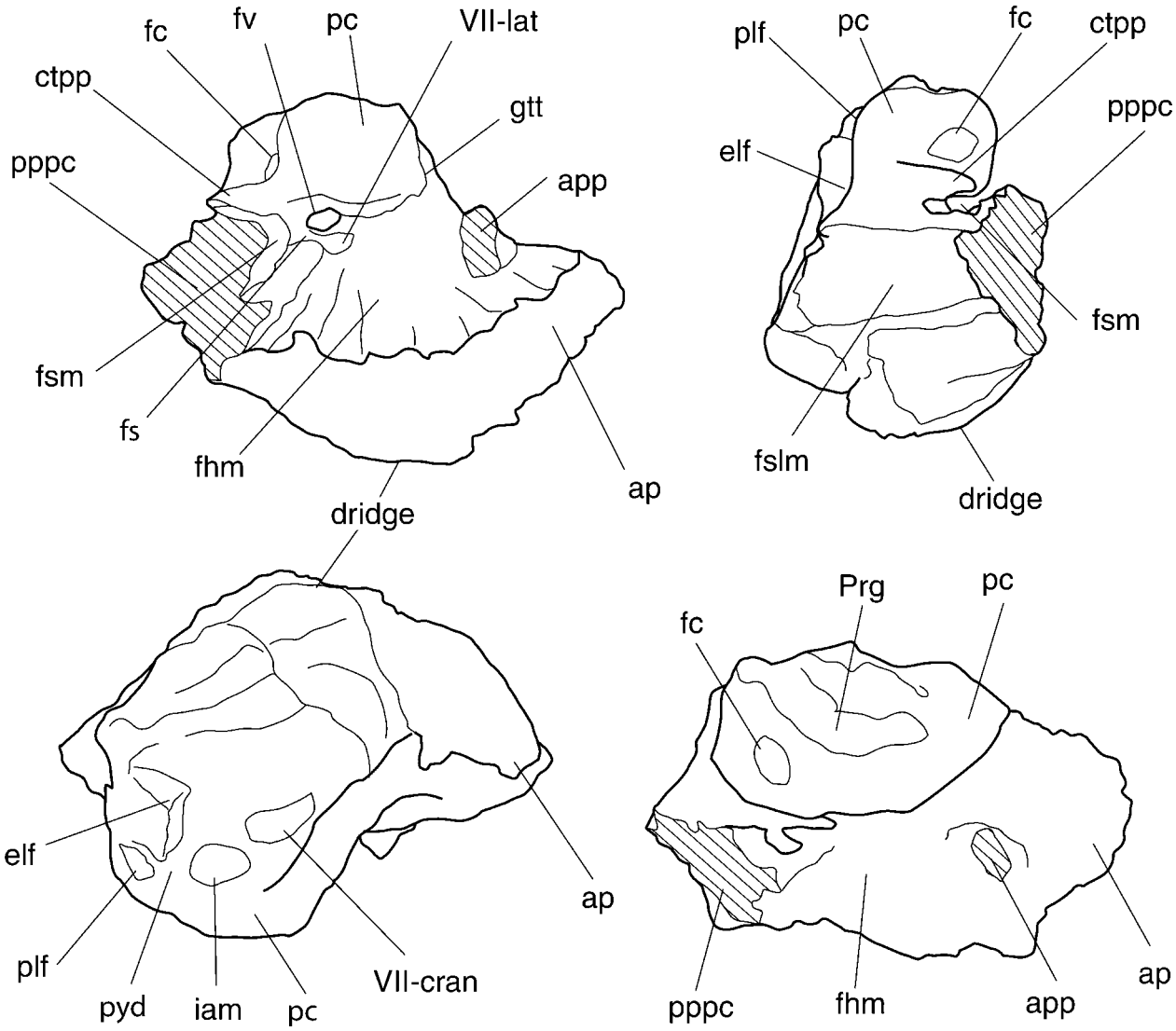

FIG. 21. Right periotic of the holotype of *Parietobalaena campiniana* (RBINS M.399-R.4018): schematic representation. A, lateral view. B, posterior view. C, medial view. D, ventral view. Not to scale. Anatomical abbreviations: ap, anterior process of periotic; app, anterior pedicle for articulation with tympanic bulla; ctpp, caudal process; dridge, dorsolateral ridge; elf, endolymphatic foramen; fc, fenestra cochleae; fhm, fossa for the head of the malleus; fs, facial nerve sulcus; fsm, stylomastoid fossa; fv, fenestra vestibuli; gtt, groove for tensor tympani; iam, internal acoustic meatus; pc, pars cochlearis; plf, perilymphatic foramen; pppc, broken emergence of posterior process of periotic; prg, promontorial groove; pyd, pyramidal process; VII-cran, endocranial foramen for cranial nerve VII (Facial); VII-lat, groove for lateral transit of cranial nerve VII (Facial).

pronounced medially and anteriorly pointed in lateral view. Posteriorly, it is in close proximity with another sharp thin crest, dorsal to the suture between the posterior process of the periotic and the external acoustic meatus.

From a dorsal point of view, the squamosal does not bulge into the temporal fossa. The dorsal part of the squamosal is missing and the basicranial structures can be seen in dorsal view owing to the wide fractures of the squamosal.

The posterior edge of the external acoustic meatus is formed by a thin crest, which is located close to the anterior surface of the posterior process of the periotic (postmeatal crest *sensu* Fordyce 1994). This crest protrudes into the cranial hiatus medially and dorsally and appears as a small, pointed, triangular lamina that covers a small part of the ventral surface of the periotic posterolaterally to the anterior process, slightly anterior to the level of the oval window. The ventromedial surface, anterior to the external acoustic meatus, is elongated anteroposteriorly and slightly concave.

Occipital. The supraoccipital is totally missing. The exoccipital is flat and vertically oriented. The posterior wall of the paroccipital process of the exoccipital is oriented obliquely (from a point located anteromedially to a point located posterolaterally). The posterolateral corner of the exoccipital is located very medially

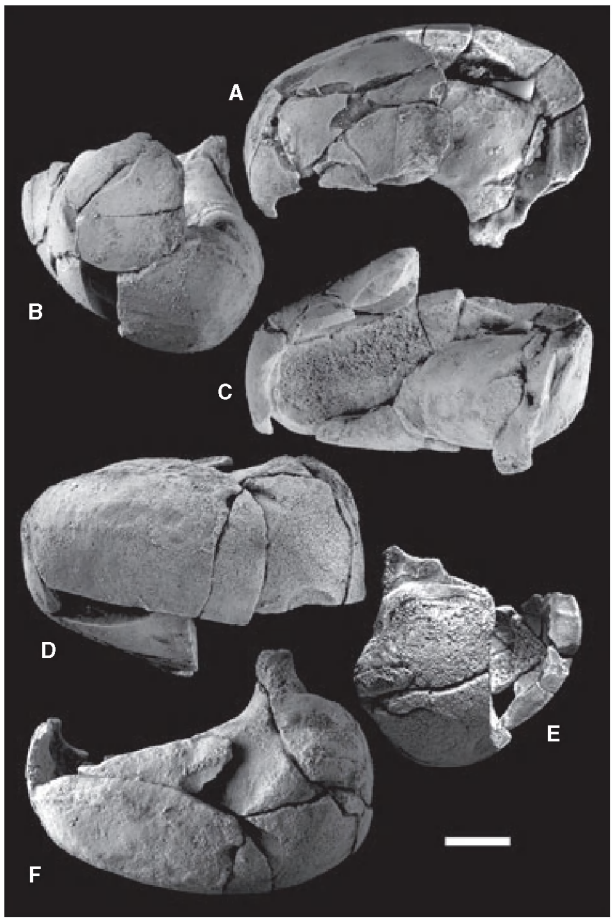

FIG. 22. Right tympanic bulla of the holotype of *Parietobalaena campiniana* (RBINS M.399-R-4018). A, lateral view (upside down). B, anterior view. C, dorsal view (anterior end on the left side). D, ventral view. E, posterior view. F, medial view. Scale bar represents 10 mm. Specimen coated with ammonium chloryde.

relative to the postglenoid process of the squamosal; it strongly protrudes posteriorly. The occipital condyles are slightly posterior to the lateral paroccipital processes. The occipital condyles are clearly separated from the paroccipital process by a groove whose surface is smooth. The condyles are hemispherical in posterior view; their ventral corners are much closer to each other than their dorsal corners. Only the ventral border of the foramen magnum is preserved; it is round and rather wide. In dorsal view, the condyles are flat-to-slightly convex. In ventral view, the basioccipital is short, wide and squared. In ventral view, it is slightly convex along both the longitudinal and the transverse axes of the skull. The descending process of the basioccipital is only a low and wide relief making contact with the posteromedial portion of the pterygoid. It is rounded-to-oval, and its ventral surface is rather rough.

Basicranium. The presphenoid is widely separated from the basisphenoid (Figs 14 and 15). It is short and wide and has a convex dorsal surface. It is located medially and posteriorly relative to the supraorbital process of the frontal. The basisphenoid is much longer and squared, and its ventral surface is longitudinally concave. Its anterior border is elevated at the middle of the bone forming the anterior edge of the sella turcica. The latter is only a slight concavity on the dorsal surface of the bone. The alisphenoid is short and protrudes from the anterolateral corner of the basisphenoid. The lateral extremity of the alisphenoid is superimposed on the pterygoid. Probably, this portion was exposed in the temporal fossa. The alisphenoid forms the anterior border of the hiatus cranicus in dorsal view.

The hiatus cranicus is broadly triangular (Fig. 19). The anterior border is rounded and rather wide; the posterolateral border is rounded and wide; the posteromedial corner is more acute. The lateral border is nearly parallel to the ventral edge of the posterior wall of the temporal fossa, and it is only a few millimetre posterior to it. The lateral and medial borders of the basicapsular fissures are straight. The anterior portion of the fissure is included within the pterygoid sinus fossa of which a part remains.

The posterior process of the periotic is still *in situ*, and its anterior end is located at the posterolateral corner of the basicapsular fissure, slightly posterior to the external acoustic meatus (Fig. 19). The latter is a rather narrow inverse V-shaped groove, which is 13.5 mm in anteroposterior diameter. It tapers laterally. The external acoustic meatus is located posterior to the postglenoid process of the squamosal.

In ventral view, the pterygoid forms a wide and long curve; it bears only a poorly developed ventral lamina, which is not large enough to cover the dorsal surface of the pterygoid sinus fossa. The foramen 'pseudo-ovale' is located between the squamosal and the pterygoid; it is elliptical.

Periotic. The rather short posterior process is still *in situ* and makes contact with the squamosal-exoccipital suture (Figs 20 and 21). It becomes slightly larger posteriorly and has a rounded posterior end. Its ventral surface is crossed by a long channel for the facial nerve (VII). Its ventral surface is transversely convex, and its length approaches the length of the anterior process and the dorsal portion of the periotic itself. The stylomastoid fossa is shallow, wide and ventromedially restricted by a low and rounded crest located at the anterior border of the posterior process. The posterior process tapers posteriorly, and its lateral surface forms an angle of 45 degrees with the anteroposterior axis of the periotic.

The anterior process is short, thick and broadly triangular in dorsal view; anteriorly, it is rounded. It is clearly separated from the central portion of the periotic by a fissure oriented dorsolaterally (Figs 20 and 21). It shows a strong posterior elevation, which makes contact with the rounded dorsal surface in cranial view. This surface bulges strongly. Dorsally, the bulge is pachyosteosclerotic. The anterior pedicle for the tympanic bulla is anteroposteriorly short and transversely oriented. The suprameatal area is very high. Its dorsomedial border is rounded and protrudes cranially. More ventrally, the suprameatal area is concave and smooth.

The internal acoustic meatus, the endocranial opening for the facial canal and the endolymphatic foramen form a triangular pattern. The endocranial opening for the facial canal is oval. The

FIG. 23. Left dentary of the holotype of *Parietobalaena campiniana* (RBINS M.399-R.4018). A, lateral view. B, dorsal view. C, medial view. Scale bar represents 100 mm.

endolymphatic foramen is long, deep and slit-like (being compressed along the anterodorsal-posteroventral axis). The internal acoustic meatus includes the tractus spiralis foraminosus and the exit for the vestibulocochlear (VIII) nerve. The meatus is separated from the endocranial opening of the facial canal by a 5.5-mm-wide crista transversa and is separated from the endolymphatic foramen by a 7.5-mm-wide pyramidal process. The endocranial opening of the facial canal (for the cranial nerve VII) is located more dorsally and anteriorly. It is connected to the anterodorsal rim of the internal acoustic meatus by a groove running over a wide crista transversa. The endocranial opening of the facial canal is oval, small (maximum diameter about 3 mm) and tube-like. The perilymphatic foramen is very small and point-like. The endolymphatic foramen is separated from the round window. The round window is oval in outline; it is medially straight and lateromedially compressed. The oval window is rather wide and oval-shaped.

The lateral opening of the facial canal is small; it opens at the level of the anterior edge of the oval window. The facial sulcus is wide and deep, and is separated from the fossa for the stapedial muscle by a fine septum. The ventral surface of the periotic, lateral to the pars cochlearis, is smooth and substantially featureless. The mallear fossa is shallow. The stylomastoid fossa is deep, lateromedially short, well roofed and with a narrow floor (3 mm wide). Its surface is smooth; the fossa is dorsoventrally low and mediolaterally short. The pars cochlearis is neither transversely nor anteroposteriorly elongated. In lateral view, it is trapezoidal. The promontorial groove is irregular, mediolaterally wide, deep and prominent. It runs all over the length of the ventral promontorial surface. Anteriorly it is restricted by a fine crest; posteriorly it is open and ends just dorsally to the round window. Its surface is rough and irregular. The tensor tympani groove is present but rather weak and continues anteroventrally on the surface of the anterior process; it shallows anteroventrally and widens anteromedially.

Tympanic bulla. Both tympanic bullae have been detached from the skull for study (Figs 22 and 23). The left bulla is markedly smaller than the right one. The bulla is short relative to its width. The bulla is substantially rounded, it is small, and its surface is very smooth and featureless. Most of the lateral and ventral walls are missing. The anterolateral corner of the bulla does not protrude laterally, and thus, the bulla is pear-shaped (Van Beneden's 'pyruliform' bulla). The opening for the Eustachian tube is rather low and transversely wide. The pedicle for the attachment of the posterior process of the periotic is slender and is located posteriorly. The tympanic cavity is deep and wide anteriorly. The medial border is nearly straight. The involucrum is rather high and robust posteriorly, sloping gradually and narrowing anteriorly. The medial keel is absent except for a weak, rounded crest on the posterior wall. Medially, the bulla is strongly rounded dorsoventrally.

Dentary. A proximal fragment of the left dentary is preserved (Fig. 24). It includes the mandibular condyle, the coronoid process and part of the ramus. Measurements are in Table S2. The

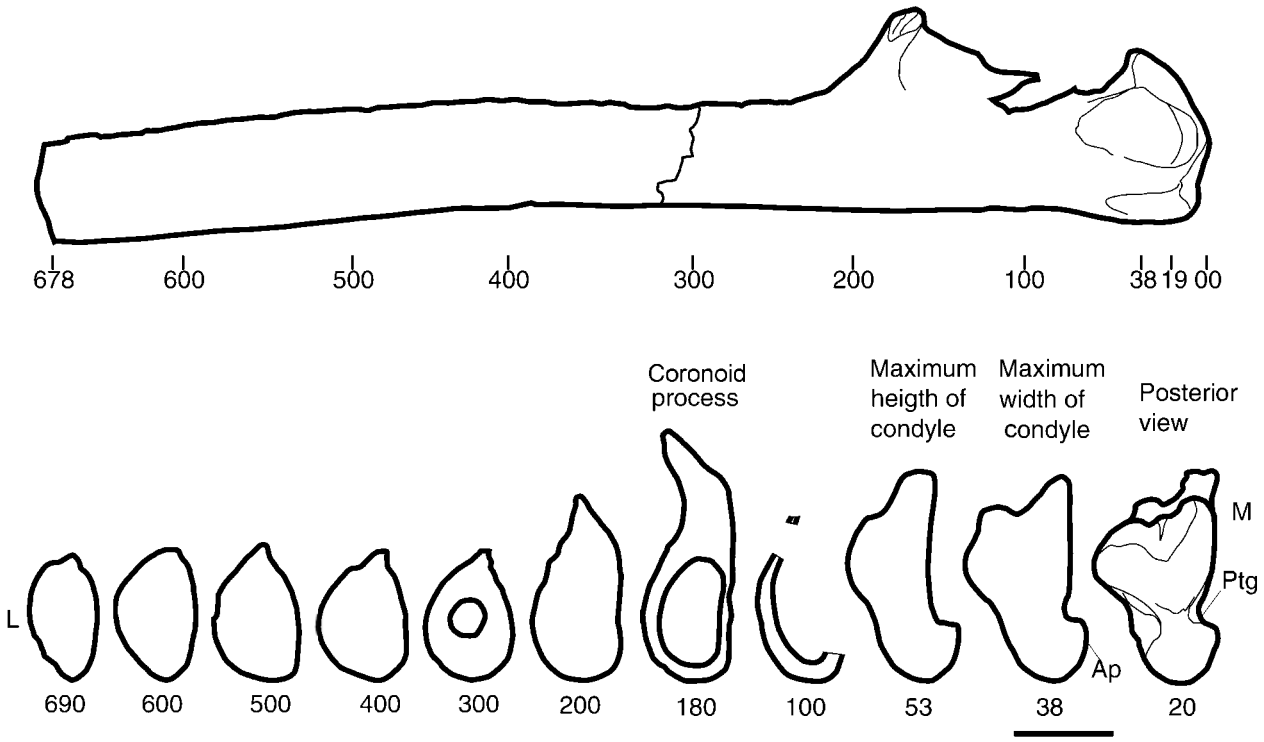

FIG. 24. Transverse sections of the left dentary of the holotype of *Parietobalaena campiniana* (RBINS M.399-R.4018). Upper row: schematic representation of left dentary; lower row, transverse sections. Thick lines represent actual bone profiles. Numbers represent distances from the posterior apex. Scale bar represents 100 mm. Abbreviations: Ap, angular process; L, lateral; M, medial; Ptg, pterygoid groove.

condyle is damaged on the lateral and dorsal sides. Its articular surface faces posteriorly and slightly dorsally. Its anterodorsal corner is higher than the dorsal border of the dentary between the condyle and the coronoid process. The angular process is approximately squared and projects slightly ventrally. It is separated from the condyle by a medial groove, which faces medially. The coronoid process is not much higher than the condyle. It bears a boss at its base. The dentary has a postcoronoid crest and fossa. The coronoid crest is short. The lateral surface of the ramus is convex transversely ventrally and anteriorly to the coronoid process. The ramus is rather straight along both anteroposterior and dorsoventral axes. The medial surface of the dentary is convex transversely (Fig. 25). The ventral border of the dentary is transversely rounded. The mandibular foramen is wide and apparently triangular. There is no mylohyoidal groove. The gingival foramina are located along the dorsal border, which is sharply edged. Only one mental foramen is preserved.

Hyoid. A small part of a hyoid bone is preserved (Fig. 26). It is probably a stylohyoid element showing a dorsoventrally convex surface and externally rounded borders.

Vertebrae. The atlas, four cervical and two thoracic vertebrae are preserved (Fig. 27). The atlas (C1) is well preserved. It is rather wide. The lateral process is high, very short, stocky and laterally convex. The posterior articular facets are dorsoventrally flat and transversely convex. The ventral border is flat with an anterior notch located between the anterior articular facets. These facets are highly concave. The third cervical vertebra is strongly damaged.

The fourth cervical vertebra is characterized by short and delicate ventral transverse processes; the epyphyses are smaller than the centrum. There are no remains of the arch and of the dorsal transverse processes. The centrum of the sixth vertebra is oval; there are no ventral transverse processes preserved and only a part of one dorsal transverse process is preserved.

The neural arch of the seventh cervical vertebra is low and wide. The dorsal transverse processes are short, dorsoventrally flat. There are no ventral transverse processes. The vertebral epyphysis is remarkably smaller than the body.

FIG. 25. Hyoid fragment? of the holotype of *Parietobalaena campiniana* (RBINS M.399-R.4018). Scale bar represents 10 mm.

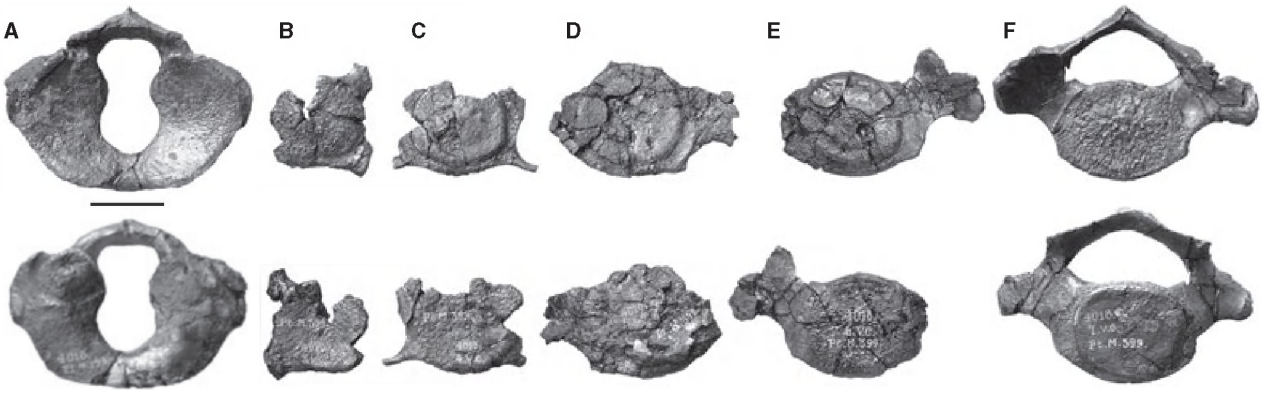

FIG. 26. Cervical vertebrae of the holotype of *Parietobalaena campiniana* (RBINS M.399-R.4018). Upper row: anterior views; lower row: posterior views. A, atlas. B–F, 3rd–7th cervical vertebrae. Scale bar represents 100 mm.

The fifth thoracic vertebra has a centrum with a straight dorsal border and a round ventral border bearing a rounded keel along the midline (Fig. 28). The transverse processes are short and stocky and display an articular facet for a single-headed rib. The transverse processes emerge from the sides of the neural arch. The neural process is squared and does not bear metapophyses.

The seventh thoracic vertebra has broadly the same characteristics as the fifth, but shows metapophyses with a lateral facet; the presence of a concavity posterior to the metapophysis is ambiguous owing to poor preservation. Measurements are provided in Table S5.

Comparisons

Rostrum. In *Parietobalaena campiniana*, the lateral process of the maxilla is short and slightly higher than the posterolateral surface of the maxilla. In Cetotheriidae and Eschrichtiidae, the lateral process of the maxilla forms a rounded antorbital notch with an anterior concavity, a typical character of these families as observed in *Piscobalaena nana*, *Mixocetus elysius* Kellogg (1934), *Cetotherium rathkii* and *Eschrichtius robustus* (True 1904; Packard *et al.* 1934; Pilleri 1986; Bouetel and de Muizon 2006). In *Diorocetus hiatus*, the anterior edge of the lateral process of the maxilla forms a distinctive and extended incisure on the posterolateral surface of the maxilla (Kellogg 1968*b*). In *Pelocetus calvertensis*, *Aglaocetus patulus* and *Isanacetus laticephalus*, the lateral process is relatively short and distally narrow as in *P. campiniana*, whereas in modern Balaenopteridae, Balaenidae and Neobalaenidae, the lateral process is very long. In *Parietobalaena palmeri* and *Titanocetus sammarinensis* Bisconti (2006), the lateral process is strongly reduced-to-absent (Kellogg 1968*d*; Bisconti 2006). The lateral process of the maxilla of *P. campiniana* closely resembles that of *Aglaocetus moreni* Kellogg (1934*a*) as the general shape of the rostrum does.

Frontal. The posterior border of the supraorbital process of the frontal of *P. campiniana* is nearly straight, and the anterior border is highly concave and the postorbital process is well developed and long. The supraorbital process of at least one specimen assigned to *Diorocetus hiatus* (USNM 16783) exhibits all these characters. *Isanacetus laticephalus* also shares these features, but in this species, the postorbital corner is not protruding externally as observed in *P. campiniana* and *D. hiatus*.

Squamosal. In dorsal view, the zygomatic process of the squamosal of *P. campiniana* is slightly divergent from the longitudinal axis of the skull, and its lateral surface is straight. This condition is observed in most archaic 'cetotheres' (*Aglaocetus moreni*, *Pelocetus calvertensis*, *Aglaocetus patulus*, *Diorocetus hiatus*, *Parietobalaena palmeri*) and in adult *Piscobalaena nana*. *Cophocetus oregonensis* Kellogg (1934*b*) *Mixocetus elysius*, *Cetotherium rathkii* and *Herpetocetus transatlanticus* have the lateral border of the zygomatic process of the squamosal parallel to the longitudinal axis of the skull, as well as living Balaenopteridae (with the exception of *Megaptera* and *Balaenoptera musculus*) and *Eschrichtius robustus*.

The zygomatic process of the squamosal of *P. campiniana* is elongated and narrow in lateral view, and the glenoid fossa of the squamosal is continuously curved. Cetotheriidae and Eschrichtiidae have a flat glenoid fossa of the squamosal with the exception of *Herpetocetus* and *Piscobalaena* (Bouetel and de Muizon 2006; Whitmore and Barnes 2008). Among early 'cetotheres', the glenoid fossa of the squamosal is flat in *Titanocetus*, *Isanacetus* and in a Japanese *Parietobalaena* sp. (Kimura *et al.* 1998; Kimura and Ozawa 2002; Bisconti 2006). In these taxa, the glenoid fossa of the squamosal is oblique because the postglenoid process protrudes more ventrally than the zygomatic process. In *Parietobalaena palmeri* and *Dioroc-*

FIG. 27. Thoracic vertebrae of the holotype of *Parietobalaena campiniana* (RBINS M.399-R.4018). A, fifth thoracic vertebra. B, seventh thoracic vertebra. Scale bar represents 100 mm.

etus hiatus, the zygomatic process is nearly horizontal and the postglenoid process nearly vertical; the glenoid fossa forms a right angle in lateral view. In these species, the zygomatic process is extremely subtle and elongate resembling very closely that of basilosaurids.

In *P. campiniana*, the foramen 'pseudo-ovale' is located between the squamosal and the pterygoid as it is observed in *Piscobalaena nana* and *Isanacetus laticephalus*. In *Peloc-etus calvertensis*, *Cophocetus oregonensis*, *Aglaocetus moreni*, *Mixocetus elysius*, *Diorocetus hiatus*, *Parietobalaena palmeri*

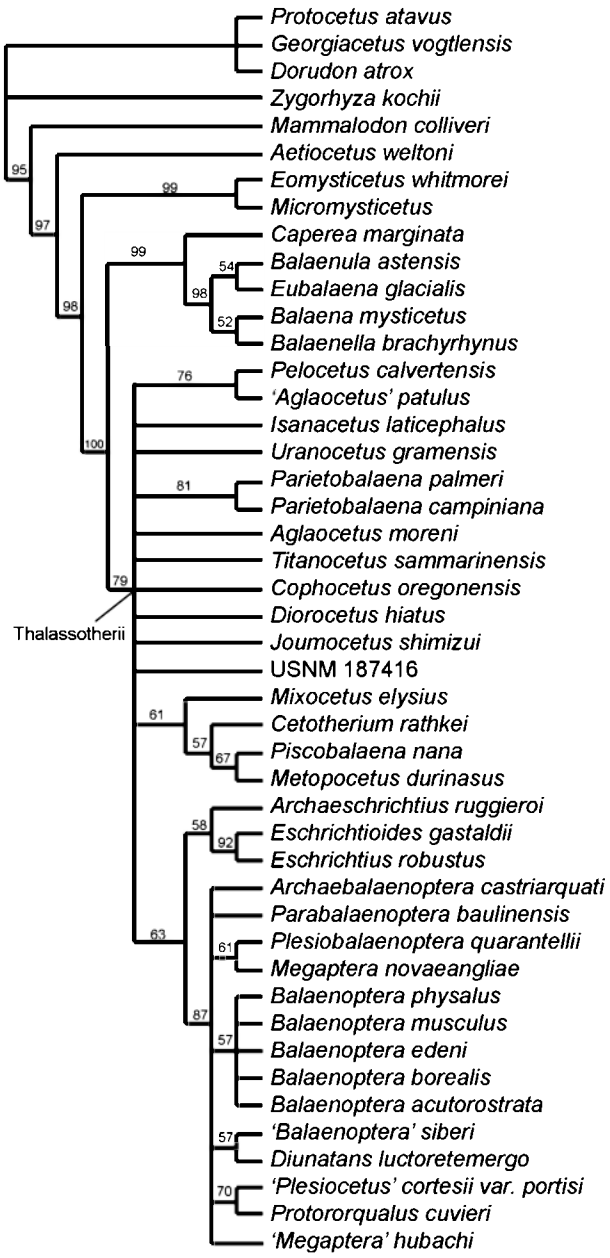

FIG. 28. Result of bootstrap analysis: 50 per cent-majority-rule consensus tree showing principal mysticete groups and the clade Thalassotherii. Tree length, 1070 steps; consistency index (CI), 0.328; homoplasy index (HI), 0.672; CI excluding uninformative characters, 0.3198; rescaled CI, 0.2076; HI excluding uninformative characters, 0.6802; retention index, 0.6328.

and *Aglaocetus patulus*, the foramen 'pseudo-ovale' is located posterior to the bifurcation of the falciform and the glenoid processes of the squamosal and is suturally connected with the squamosal-pterygoid suture.

In *Parietobalaena campiniana*, the posterolateral corner of the temporal fossa is rather acute resembling that of Cetotheriidae (with the exception of *Piscobalaena nana*). In Cetotheriidae, the squamosal bulges into the temporal fossa, forming an outer convexity medial to the zygomatic process; in the other archaic 'cetotheres', the ventral border of the posterior wall of the temporal fossa is uniformly convex, forming a wide concavity only approaching the emergence of the zygomatic process.

Periotic. The periotic of *Parietobalaena campiniana* differs from that of *Pelocetus calvertensis*, *Isanacetus laticephalus*, *Cophocetus oregonensis*, *'Aulocetus' calaritanus* Capellini (1899), *Idiocetus longifrons* Van Beneden (1880) (RBINS M.719-R.769), *Mesocetus latifrons* Van Beneden (1880) (RBINS M.567-R.198), in that the endocranial opening for the Facial canal is well separated from the internal acoustic meatus and is prolonged into a long and narrow fossa that reaches the anterodorsal border of the internal acoustic meatus. *Parietobalaena campiniana* shares this trait with *Mesocetus longirostris* (RBINS M.548-R.1539), *Amphicetus later* Van Beneden (1880) (M.575-R.313), *Heterocetus affinis* (RBINS M.605-R.301), *Parietobalaena palmeri*, *Diorocetus hiatus*, *Herpetocetus scaldiensis, H. transatlanticus, H. bramblei*, *Piscobalaena nana* and *Metopocetus durinasus*. This character is also observed in the periotic of newborn living balaenopterids (Bisconti 2001) and is part of the intraspecific variation in the living fin whale, *Balaenoptera physalus* (Bisconti and Bosselaers pers. obs.).

In *Herpetocetus scaldiensis, H. transatlanticus, H. bramblei*, *Metopocetus durinasus* and *Piscobalaena nana* (Cetotheriidae), the dorsomedial border of the suprameatal area is rounded and rather high; this character is shared with *Parietobalaena campiniana*, *Amphicetus later* (M.598) and *Idiocetus laxatus* (RBINS M.712). However, in *P. campiniana*, the dorsal surface of the periotic is strongly elevated and forms a high dome. The superior surface of the anterior process descends anteriorly from this dome. The anterior process of *P. campiniana* is short and resembles that of *Parietobalaena palmeri* and *Heterocetus affinis* (RBINS M.605a).

The dorsal surface of the periotic of *P. campiniana* reaches its highest point anteriorly to the endocranial opening of the facial canal. Whereas in *P. calvertensis*, *I. laticephalus*, *'A.' calaritanus* and *H. affinis* (RBINS M.605b), the highest point of the superior surface is located on the exactly dorsally to the internal acoustic meatus, whereas it is located more anteriorly in *Mesocetus longirostris* (RBINS M.548), *M. latifrons* (RBINS M.567), *Diorocetus hiatus, Thinocetus arthritus*, *Piscobalaena nana*, *Metopocetus durinasus*, *Herpetocetus transatlanticus* and *Amphicetus later* (M.598).

Discussion

The comparative and the phylogenetic analysis (see below) show that the specimens RBINS M.399-R.4018,

RBINS M.2010 and RBINS M.2011 are morphologically very similar to *Parietobalaena palmeri*. This supports their inclusion within the genus *Parietobalaena*. The Belgian specimen differs from *P. palmeri* substantially in the structure and robustness of the supraorbital process of the frontal and the morphology of the angular process of the dentary. In fact, in RBINS M.399-R.4018, the postorbital corner is much stronger and does not project clearly posteriorly as seen in *P. palmeri*. Moreover, the supraorbital process of the frontal is longitudinally longer and more robust than that of *P. palmeri*. Given that the degree of intraspecific morphological variation in these features has been well figured by Kellogg (1968*d*), the observed differences can be regarded as diagnostic of genetic differences supporting our view that RBINS M.309/R. 4018 is a different species of *Parietobalaena*, namely *P. campiniana*. We will discuss more about this species in the phylogenetic analysis section.

PHYLOGENETIC ANALYSIS

Goals

The taxonomic revision of *Isocetus depauwi* and the discovery of a new mysticete taxon in the Miocene of the southern North Sea provide new material for a detailed study of the phylogenetic relationships of fossil mysticetes, especially the basal thalassotherians. In this paper, we present a new, detailed morphological analysis of mysticete phylogeny with the following goals: (1) to understand the phylogenetic relationships of *Parietobalaena campiniana*; (2) to test the hypothesis of monophyly of Cetotheriidae *s.s.* and Cetotheriidae *s.l. sensu* Whitmore and Barnes (2008) and Kimura and Hasegawa (2010), (3) to understand the relationships of the modern mysticete families and the archaic cetotheriids and 'cetotheres', and (4) to assess the degree of agreement of the branching order and the stratigraphic occurrence of the taxa included in the analysis.

Material

Our analysis is based on the comparative study of a number of recent and fossil specimens representing all the known mysticete radiations (see Supporting Information published online in the website of *Palaeontology* for a complete list of the examined specimens, character list and matrix). The information gathered from these specimens is supplemented by taxa for which detailed descriptions are available in the scientific literature as provided in the online Supplementary Information. In total, we scored character states for 46 taxa, including four outgroup species (the archaeocetes *Protocetus atavus* Fraas (1904), *Georgiacetus vogtlensis* Hulbert *et al.* (1996) *Dorudon atrox* and *Zygorhiza kochii*) and 42 ingroup mysticete species. We also included in our analysis the specimen USNM 187416 from the Calvert Formation, Bed 13 at Parker Creek, Maryland, previously assigned to *Parietobalaena palmeri*.

Methods

The 246 characters used in the present phylogenetic analysis were mainly selected based on the morphology of the skeleton (244) and the baleen (2). Character states were selected on the basis of our observations and of previous studies (McLeod *et al.* 1993; Geisler and Luo 1996, 1998; Bisconti 2000, 2005, 2007*a*, *b*, 2008; Sanders and Barnes 2002*a*, *b*; Kimura and Ozawa 2002; Geisler and Sanders 2003; Deméré *et al.* 2005, 2008; Steeman 2007, 2010). The character list is presented in the online Supporting Information, together with the matrix used in the phylogenetic analysis.

The matrix was treated by PAUP 4.0b10 (Swofford 2002); character states were unordered and unweighted under the ACCTRAN character states optimization. The tree–bisection–reconnection (TBR) algorithm, with one tree being held at each step during stepwise addition, was used to find the most parsimonious cladograms. Character support at nodes was assessed by a bootstrap analysis with 1000 replicates. A randomization test was performed to evaluate the distance of the cladograms resulting from the TBR search and 10 000 cladograms sampled equiprobably from all the possible cladograms deriving from the matrix.

To evaluate the degree of agreement of the branching order of the cladograms resulting from TBR search and the stratigraphic occurrence of the taxa, the stratigraphic consistency index (SCI) of Huelsenbeck (1994) was calculated (see Bisconti 2007*a*, *b*, 2008 for a discussion on the SCI). Stratigraphic data were obtained mainly from the Paleobiology Database compiled by Uhen (2010).

Results

The TBR search resulted in 216 trees whose strict consensus is presented in Figure 2 (tree statistics are provided in the corresponding caption). These results confirm the monophyly of Mysticeti Flower, 1864, Chaeomysticeti Mitchell (1989), Balaenomorpha Geisler and Sanders (2003), Eomysticetoidea Sanders and Barnes (2002*b*), Balaenoidea Gray (1825), Balaenidae Gray (1825), Eschrichtiidae Ellerman and Morrison-Scott (1951), Balaenopteridae Gray (1864) and Cetotheriidae Brandt (1872). The assem-

blage including Cetotheriidae and basal thalassotherians (the latter include *Joumocetus shimizui, Parietobalaena palmeri, Parietobalaena campiniana, Diorocetus hiatus, Pelocetus calvertensis, Uranocetus gramensis* Steeman (2009), *'Aglaocetus' patulus, Isanacetus laticephalus*) is paraphyletic.

The genus *'Aglaocetus'* is polyphyletic because the two species *'Aglaocetus' patulus* and *Aglaocetus moreni* do not form a clade. This conclusion supports the polyphyly of *Aglaocetus* found by Marx (2011). For these reasons, and for priority reasons, we conclude that a new generic name is necessary for *'Aglaocetus' patulus*.

In the branching order of the cladogram (Fig. 2), Eomysticetoidea is the sister group of Balaenomorpha. The most basal branching Balaenomorpha are Balaenoidea (Balaenidae and Neobalaenidae) and basal thalassotherians including *Joumocetus shimizui*, *Parietobalaena palmeri* and *P. campiniana*. *Parietobalaena campiniana* and *P. palmeri* form a monophyletic clade. Broad-nosed thalassotherians including *Pelocetus calvertensis*, *'Aglaocetus' patulus* and *Uranocetus gramensis* form a monophyletic group that is the sister group of *Isanacetus laticephalus* and the other more derived mysticetes. *Isanacetus laticephalus* is the sister group of a wide radiation of mysticetes including Cetotheriidae, Eschrichtiidae, Balaenopteridae and advanced thalassotherians such as *Cophocetus oregonensis*, *Titanocetus sammarinensis* and *Aglaocetus moreni*. *Diorocetus hiatus* is the sister group of Cetotheriidae (including *Cetotherium rathkii, Metopocetus durinasus, Piscobalaena nana* and *Mixocetus elysius*). We maintain *Diorocetus hiatus* outside Cetotheriidae because it lacks key characters of this family such as the strongly protruded posteromedial corners of the maxilla and the morphology of the vertex. Eschrichtiidae is the sister group of Balaenopteridae, confirming previous studies (Deméré *et al.* 2005; Marx 2011) and *contra* Bisconti (2007*a*, *b*, 2008) and Steeman (2007).

The randomization test showed that the length of the trees resulting from the TBR search was significantly lower (tree length = 912 steps) than the mean length of 10 000 cladograms sampled equiprobably from all the trees that can be generated from the matrix (mean length = 2009.79 steps) ($p < 0.0001$).

The SCI of the strict consensus tree of Figure 2 is 0.545. This low value depends in large part on the lack of resolution in the balaenopterid clade (only four clades are present instead of 12). This lowers the number of clades that can be evaluated in stratigraphic terms. The number of stratigraphically consistent nodes is 24 on a total of 44 expected nodes.

The consistency index, retention index and homoplasy index all suggest that high levels of homoplasy are present in the phylogeny of Figure 2. This observation is confirmed by the 50 per cent-majority-rule strict consensus tree presented in Figure 28 where most of the clades collapsed into unresolved polytomies. High bootstrap values (from 80 to 100 per cent) are recorded for Mysticeti (95 per cent), Chaeomysticeti (98 per cent), Balaenomorpha (100 per cent), Balaenoidea (99 per cent), Balaenidae (98 per cent) and Balaenopteridae (87 per cent). Thalassotherii was slightly below the threshold, having a bootstrap support value of 79 per cent. Cetotheriidae and Eschrichtiidae received lower support values (61 and 58 per cent, respectively). The monophyly of Eschrichtiidae + Balaenopteridae was supported by a value of 63 per cent; despite the low value, the bootstrap analysis supported the validity of Balaenopteroidea *sensu* Deméré *et al.* (2005) including Eschrichtiidae + Balaenopteridae. A value of 76 per cent was found to support the monophyly of the *Pelocetus calvertensis* + *'Aglaocetus' patulus* clade. Also in the bootstrap tree, *Parietobalaena campiniana* forms a clade with *P. palmeri* (81 per cent).

DISCUSSION

Phylogenetic relationships of archaic mysticetes

The phylogenetic relationships of archaic 'cetothere' mysticetes are a hot topic. Different studies resulted in the wealth of solutions reviewed by Kimura and Hasegawa (2010). The osteology of these mysticetes is difficult to interpret in evolutionary terms because 'cetotheres' have been largely identified as those mysticetes that do not exhibit the apomorphies of the living families and became a taxonomic basket lacking clear defining characters (Fordyce and de Muizon 2001).

In the effort to clarify the diversity and taxonomy of these whales, the results of some authors (Bouetel and de Muizon 2006; Steeman 2007; Bisconti 2008; Whitmore and Barnes 2008) converged towards the definition of a peculiar group of archaic mysticetes (i.e. Cetotheriidae *s.s.*) which exhibit long ascending process of the maxilla obliterating the interorbital region of the frontal, anteriorly diverging lateral borders of the ascending process of the maxilla, short and relatively wide parietal exposure at vertex, short supraorbital process of the frontal, anteriorly concave antorbital notch and strong protrusion of squamosal into the temporal fossa. It is widely accepted that Cetotheriidae *s.s.* includes *Cetotherium rathkii*, *Metopocetus durinasus*, *Nannocetus eremus* Kellogg (1929), *Mixocetus elysius*, *Herpetocetus scaldiensis*, *H. transatlanticus*, *H. bramblei* Whitmore and Barnes (2008), and *Piscobalaena nana* (Bouetel and de Muizon, 2006; Whitmore and Barnes, 2008).

The so-called Cetotheriidae *incertae sedis* by Whitmore and Barnes (2008) and Mysticeti *incertae sedis* by Uhen *et al.* (2008) include well-preserved mysticetes such as *Isanacetus laticephalus*, *Parietobalaena palmeri*, *Diorocetus*

hiatus, *Pelocetus calvertensis*, *Aglaocetus moreni*, *'Aglaocetus' patulus*, *Cophocetus oregonensis* and *Titanocetus sammarinensis* (according to Bisconti 2006). These 'cetotheres' have been variously included in phylogenetic analyses by Kimura and Ozawa (2002), Deméré *et al.* (2005, 2008), Bouetel and de Muizon (2006), Steeman (2007), Bisconti (2008), Kimura and Hasegawa (2010), and Marx (2011) with two main results: in one result, these 'cetotheres' represent a paraphyletic assemblage (Kimura and Ozawa 2001; Deméré *et al.* 2005; Bouetel and de Muizon 2006; Bisconti 2008; Marx 2011); in a variant of this result, they form a number of family- or subfamily-rank clades (Steeman 2007); in the other result, they form a monophyletic group.

To overcome this problem, we performed a phylogenetic analysis based on one of the most comprehensive osteological analyses of the mysticetes ever attempted up to now. Our conclusion supports the monophyly of Cetotheriidae and the paraphyletic status of the other 'cetotheres'. Contrary to Steeman's (2007) results, we did not find morphological support for Pelocetidae, Aglaocetidae and Diorocetidae; our results confirms the analysis performed by Marx (2011) that did not find support for the systematic revisions of Steeman (2007). Rather, we found support for a clade formed by broad-nosed 'cetotheres' only, including *Pelocetus calvertensis*, *'Aglaocetus' patulus* and *Uranocetus gramensis*. Also Marx (2011), in one of his analyses, found a clade including *Pelocetus* and *Uranocetus*. These mysticetes share a transversely narrow crista transversa, making it very close the endocranial opening of the facial canal and cavity with tractus spiralis foraminosus and foramen singulare. Our results suggest that this character should be interpreted as a unique reversal occurring in this lineage. They also share wide maxillae and a long lateral process of the maxilla. *Pelocetus* and *'A.' patulus* share the lack of a sagittal crest on the vertex-exposed parietal and straight lateral borders of the supraoccipital in dorsal view. However, we consider the support and bootstrap confirmation too low to name the clade. Support for Pelocetidae, Aglaocetidae and Diorocetidae *sensu* Steeman (2007) was lacking also from the bootstrap results. Because we were unable to find such a support, we must consider these families nomina dubia.

We found a high bootstrap support value (79 per cent) for a wide group including Eschrichtiidae, Cetotheriidae, Balaenopteridae and all the 'cetotheres'; we name this clade Thalassotherii and present the morphological support for it. Two distinct morphological transformations occurred within Thalassotherii that changed the primitive conditions of the group in two smaller clades included within it: (1) the evolution of highly interdigitated vertex through posterior projection of posteromedial elements of the rostrum on the interorbital region of the frontal (Cetotheriidae, Eschrichtiidae and Balaenopteridae) and (2) the secondary inclusion of the endocranial opening of the facial canal within the internal acoustic meatus as seen in Balaenopteridae and in the clade including *Pelocetus calvertensis*, *Uranocetus gramensis* and *'Aglaocetus' patulus*.

From our results, Eschrichtiidae is the sister group of Balaenopteridae and Cetotheriidae is the sister group of Eschrichtiidae; this result is in accord with Deméré *et al.* (2005) and Marx (2011) but it is *contra* Bisconti (2007*a*, *b*, 2008, 2010) and Steeman (2007). Eschrichtiidae and Balaenopteridae share the suite of morphological characters presented in Table 1 and their monophyly is confirmed also by the bootstrap analysis of Figure 28 (63 per cent). The sister group of Eschrichtiidae and Balaenopteridae should be searched among advanced thalassotherians similar to *Cophocetus oregonensis*, *Aglaocetus moreni* and *Titanocetus sammarinensis*. Our results suggest that Cetotheriidae (both *s.s.* and *s.l.*) is not sister group of *Caperea* + Balaenopteroidea, a result found by Marx (2011). The position of *Caperea* is still controversial as confirmed by the results published recently by Marx (2011) and Geisler *et al.* (2011). In the latter study, *Caperea* is the sister group of Balaenidae only in the morphological partition of the dataset, but it is more closely related to Balaenopteridae and Eschrichtiidae if gene sequences are taken into account. Our results confirm the traditional view of *Caperea* as closely related to Balaenidae.

In conclusion, we did not find support for the superfamily Cetotherioidea Steeman (2007) (including Cetotheriidae, Eschrichtiidae, *Cetotherium megalophysum*, *Mixocetus* and *'Mesocetus' argillarius*).

Our results are in broad agreement with the recent large-scale analysis published by Marx (2011), which found most of the clades that we found, including Thalassotherii. In Marx's (2011) results, 'cetotheres' are paraphyletic and Cetotheriidae are monophyletic. Details of

TABLE 1. Morphological support for Balaenopteroidea *sensu* Deméré *et al.* (2005) including Eschrichtiidae and Balaenopteridae.

Transformation	Apomorphy description
Character 21 (0 → 1)	Lateral border of ascending process and posterior border of maxilla form a approximately right or acute angle
Character 46 (1 → 2)	Supraorbital process of frontal abruptly depressed from interorbital region of frontal
Character 50 (1 → 2)	Posterior orientation of anterior border of supraorbital process of frontal
Character 51 (1 → 2)	Ascending temporal crest reduced to a line

the phylogenetic relationships are different; among these differences, the most striking is the sister group relationship of *Caperea marginata* Gray (1864) with Balaenopteridae, which makes the Balaenoidea paraphyletic and the basal position of *Diorocetus hiatus* in the whole thalassotherian radiation. Marx (2011) analysed 150 morphological characters in 55 taxa while we analysed 246 characters in 46 taxa focusing on osteology. In future studies, we will try to include as many taxa as Marx in our data matrix, which covered the morphological variation of mysticetes in a fuller way.

Our study and the one of Marx's (2011) were the most inclusive phylogenetic works on mysticetes and retrieved similar topologies. This suggests that the inclusion of more characters and more taxa in large-scale phylogenetic analyses of the mysticetes should converge towards topologies similar to those published in the present work and in Marx (2011). Our results differ from those of Marx (2011) in the following points: (1) we found a morphologically primitive cetothere group including *Joumocetus* and *Parietobalaena*, a monophyletic group including *Pelocetus*, *Uranocetus*, *'Aglaocetus' patulus* (Marx found that *Pelocetus* and *Uranocetus* are closely related together with *'Aglaocetus' moreni*); (2) we found that *Diorocetus hiatus* is the sister taxon of Cetotheriidae *s.s.* (Marx found that *D. hiatus* is the most basal thalassotherian species); (3) we found that three advanced cetotheriid *s.l.* species (*Titanocetus sammarinensis*, *'Aglaocetus' moreni* and *Cophocetus oregonensis*) were closely related to Balaenopteroidea (Marx found that these three species are basal in the radiation of Thalassotherii; (4) we found that *Caperea marginata* is closely related to Balaenidae (Marx found it is more closely related to Balaenopteroidea); (5) we found different arrangement of branches in the balaenopterid lineage (in particular, in our study, *Parabalaenoptera* is a basal balaenopterid species, and *'Balaenoptera' siberi* is not related to *B. musculus*). We expect that the inclusion of the new taxa currently under description will help in resolving these conflicts in the next few years.

Phylogenetic relationships of Parietobalaena campiniana

The TBR algorithm found that *Parietobalaena campiniana* and *Parietobalaena palmeri* form a monophyletic group highly supported by the bootstrap analysis. This clade (coincident with the genus *Parietobalaena*) is supported by character 9 ($0 \rightarrow 1$) (lateral process of maxilla short-to–absent), 91 ($0 \rightarrow 1$) (presence of a lateral fossa on the squamosal) and 146 ($0 \rightarrow 1$) (anterior process of periotic very short-to-absent).

The presence of *Parietobalaena* in southern North Sea was suggested also by Steeman (2010) based on a taxonomic revision of the 'cetotheres' from Belgium. Steeman (2010) founded her conclusion on the basis of ear bone morphology of other specimens and substantially discarded all the other available evidence. It is true that the thalassotherian species described by Van Beneden are largely fragmentary, and, in most cases, they are not useful for accurate descriptions and taxonomy. However, in some cases, skull portions and postcranial elements may be informative enough to allow a reliable taxonomic assignment. Therefore, they should be taken into consideration at least until one demonstrates they are anatomically and taxonomically uninformative. In our opinion, the discussion on the species established by Van Beneden should include all the available evidence. For this reason, we still retain the taxa established by that Belgian palaeontologist at the genus level until a complete taxonomic revision is made. As far as the genus *Parietobalaena* is concerned, in the discussion of the emended diagnosis of this genus we state that Belgian *Parietobalaena*-like forms (i.e. *Heterocetus affinis* and *'Idiocetus' laxatus*) display morphological characters that make their inclusion in the genus *Parietobalaena* at least questionable. A complete revision of the Belgian 'cetotheres' is thus necessary to circumvent this *impasse*.

The genus *Parietobalaena* is known from the Early Miocene of Maryland (Whitmore 1994), Japan (Kimura *et al.* 1998) and the southern North Sea. It shows a northern distribution that includes the North Atlantic and at least the western North Pacific. More detailed taxonomic revision of Miocene thalassotherians and more comprehensive phylogenetic analysis are necessary to get a better understanding of the palaeobiogeography of this genus.

CONCLUSIONS

The taxonomic revision of *Isocetus depauwi* provided a wealth of new information on the taxonomy and phylogeny of mysticetes. In fact, we found enough morphological data to support the validity of *Isocetus*, but additional material is necessary to better assess its phylogenetic relationships. In the process of the revision, we discovered the new species *Parietobalaena campiniana* based on a partial skeleton previously assigned to *I. depauwi*. This is the first find of *Parietobalaena* in the southern North Sea based on material from different parts of the skeleton.

The new data obtained in the present revision, together with a new and thorough analysis of the skeletal morphology of mysticetes, provided the basis for a new, large-scale phylogenetic study of baleen-bearing whales, which resulted in the discovery of a large superfamily-rank clade that we named Thalassotherii that includes Cetotheriidae *s.l.*, Cetotheriidae *s.s.*, Eschrichtiidae and Balaenopteridae. The new clade is diagnosed by characters observed in the ear bones, the supraoccipital and the dentary.

Acknowledgements. The authors wish to thank Annelise Folie and Etienne Steurbaut (both at RBINS) for their kind help in accessing and managing specimens under their care; Klaas Post (Natuurhistorisch Museum Rotterdam) for financial support to M. B. and for his contribution to the discussion; and David Bohaska (USNM) and Nancy Simmons (AMNH) for granting access to specimens under their care. Oliver Hampe and an anonymous reviewer greatly improved the quality and the clarity of this paper, and we want to express our gratitude to them. We are indebted to the kindness and professionality of the editors of *Palaeontology* who handled our manuscript: David Polly and Svend Stouge; we want to thank them very much for their efforts. We also want to thank W. Miseur (RBINS) for the quality of the pictures presented in Figures 20 and 22. This research received support from the Synthesys Project http://www.synthesys.info/, which is financed by the European Community Research Infrastructure Action under the FP 7 (BE-TAF Project n. 305 developed by M. B.); additional support was granted by a Collection Study Grant funded to M. B. by AMNH in 2005. In this paper, O. L. provided historical and stratigraphic data and contributed to the discussion; M. Boss. prepared the specimens, provided the illustrations, the measurements, the descriptions of the referred materials and contributed to the comparisons and discussion; M. B. provided the descriptions, comparisons, phylogenetic analysis, contributed to the discussion and wrote the paper.

Editor. P. David Polly

SUPPORTING INFORMATION

Additional Supporting Information may be found in the online version of this article:

Appendix S1. Supplementary Material to Taxonomic revision of *Isocetus depauwi* (Mammalia, Cetacea, Mysticeti) and the phylogenetic relationships of archaic 'cetothere' mysticetes.

Fig. S1. Indeterminate specimens previously assigned to *Isocetus depauwi*.

Fig. S2. Indeterminate specimens previously assigned to *Isocetus depauwi*.

Fig. S3. RBINS M.2010. Isolated right periotic referred to *Parietobalaena campiniana*.

Fig. S4. RBINS M.2011. Partial left squamosal tentatively referred to *Parietobalaena campiniana*.

Table S1. Measurements of tympanic bullae.

Table S2. Measurements of the dentaries of the lectotype of *Isocetus depauwi* (M.396-R.370) and the holotype of *Parietobalaena campiniana* (M.399-R.4018).

Table S3. Measurements of the vertebrae of the lectotype of *Isocetus depauwi* (RBINS M.396-R.370). Data in mm.

Table S4. Measurements of the skull of the holotype of *Parietobalaena campiniana* (M.399-R.4018).

Table S5. Measurements of the vertebrae of the holotype of *Parietobalaena campiniana* (RBINS M.399-R.4018).

Table S6. Measurements of RBINS R.920 (Mysticeti, gen. et sp. indet.).

Table S7. Measurements of RBINS R.1556 and R.1557 (Mysticeti, gen. et sp. indet.).

Table S8. Measurement of five non-numbered vertebrae previously assigned to *Isocetus depauwi*.

Please note: Wiley-Blackwell are not responsible for the content or functionality of any supporting materials supplied by the authors. Any queries (other than missing material) should be directed to the corresponding author for the article.

REFERENCES

ABEL, O. 1938. Vorlaeufige mitteilungen ueber die revision der fossilen mystacoceten aus dem Tertiaer Belgiens. *Bulletin du Musée royal d'Histoire naturelle de Belgique*, **14**, 1–34.

ANDREWS, C. W. 1906. *A descriptive catalogue of the Tertiary Vertebrata of the Fayum, Egypt*. British Museum of Natural History, London, 324 pp.

BARNES, L. G. and MCLEOD, S. A. 1984. The fossil record and phyletic relationships of gray whales. 3–32. *In* JONES, M. L., LEATHERWOOD, S. and SWARTZ, S. (eds). *The gray whale*. Academic Press, Orlando, 600 pp.

BENEDEN, P.-J. VAN 1880. Les mysticètes à courts fanons des sables des environs d'Anvers. *Bulletin de l'Académie Royale des Sciences, des Lettres et des Beaux-arts de Belgique*, **50**, 11–25.

—— 1886. Description des ossements fossiles des environs d'Anvers. Genres: Amphicetus, Heterocetus, Mesocetus, Idiocetus & Isocetus. *Annales du Musée Royal d'Histoire Naturelle de Belgique*, **13**, 1–139, plus Atlas.

—— and GERVAIS, P. 1868. *Osteographie des Cetaces vivants et fossiles*. Atlas, Arthus Bertrand, Paris, 64 pls.

BISCONTI, M. 2000. New description, character analysis and preliminary phyletic assessment of two Balaenidae skulls from the Italian Pliocene. *Palaeontographia Italica*, **87**, 37–66.

—— 2001. Morphology and postnatal growth trajectory of rorqual petrosal. *Italian Journal of Zoology*, **68**, 87–93.

—— 2003. Evolutionary history of Balaenidae. *Cranium*, **20**, 9–50.

—— 2005. Skull morphology and phylogenetic relationships of a new diminutive balaenid from the lower Pliocene of Belgium. *Palaeontology*, **48**, 793–816.

—— 2006. *Titanocetus*, a new baleen whale from the Middle Miocene of northern Italy (Mammalia, Cetacea, Mysticeti). *Journal of Vertebrate Paleontology*, **26**, 344–364.

—— 2007*a*. Taxonomic revision and phylogenetic relationships of the rorqual-like mysticete from the Pliocene of Mount Pulgnasco, northern Italy (Mammalia, Cetacea, Mysticeti). *Palaeontographia Italica*, **91**, 85–108.

—— 2007*b*. A new basal balaenopterid from the Early Pliocene of northern Italy. *Palaeontology*, **50**, 1103–1122.

—— 2008. Morphology and phylogenetic relationships of a new eschrichtiid genus (Cetacea: Mysticeti) from the Early Pliocene of northern Italy. *Zoological Journal of the Linnean Society*, **153**, 161–186.

—— 2010. A new balaenopterid whale from the Late Miocene of the Stirone River, northern Italy (Mammalia, Cetacea, Mysticeti). *Journal of Vertebrate Paleontology*, **30**, 943–958.

—— and VAROLA, A. 2006. The oldest eschrichtiid mysticete and a new morphological diagnosis of Eschrichtiidae (Gray

Whales). *Rivista Italiana di Paleontologia e Stratigrafia*, **112** (3), 1–11.

BOSSELAERS, M. and POST, K. 2010. A new fossil rorqual (Mammalia, Cetacea, Balaenopteridae) from the Early Pliocene of the North Sea, with a review of the rorqual species described by Owen and Van Beneden. *Geodiversitas*, **32**, 331–363.

BOUETEL, V. and DE MUIZON, C. 2006. The anatomy and relationships of *Piscobalaena nana* (Cetacea, Mysticeti), a Cetotheriidae s.s. from the early Pliocene of Peru. *Geodiversitas*, **28**, 319–395.

BRANDT, J. F. 1872. Über eine neue Classification der Bartenwale (Balaenoidea) mit Berücksichtigung der untergegangenen Gattungen derselben. *Bulletin de l'Academie imperiale des Sciences, St. Pétersburg*, **3**, 113–124.

—— 1873. Untersuchungen über die fossilen und subfossilen cetaceen Europa's. *Mémoires de L'Académie Impériale des Sciences de Saint-Petersbourg, Series 7*, **20**, 1–372.

BRISSON, A. D. 1762. *Regnum animale in classes IX Distributum, sive synopsis methodica. Lugdum Batarorum, apud.* Theodorum Haak, Leiden, 384 pp.

CARROLL, R. L. 1988. *Vertebrate paleontology and evolution*. Freeman, New York, 698 pp.

CARUS, C. G. 1847. Resultate geologischer, anatomischer und zoologischer untersuchungen über das unter den Namen Hydrarchos von Dr. A. C. Koch zuerst nach Europa gebrachte und in Dresden augestelte grofse fossile Skelett, Jena, 15 pp.

COPE, E. D. 1896. Sixth contribution to the knowledge of the marine Miocene fauna of North America. *Proceedings of the American Philosophical Soceity*, **35**, 139–146.

DEMÉRÉ, T. A., BERTA, A. and MCGOWEN, M. R. 2005. The taxonomic and evolutionary history of fossil and modern balaenopteroid mysticetes. *Journal of Mammalian Evolution*, **12**, 99–143.

——MCGOWEN, M. R., BERTA, A. and GATESY, J. 2008. Morphological and molecular evidence for a stepwise evolutionary transition from teeth to baleen in mysticete whales. *Systematic Biology*, **57**, 15–37.

ELLERMAN, J. A. and MORRISON-SCOTT, J. C. S. 1951. *Checklist of Palaeartic and Indian mammals 1758–1946*. British Museum (Natural History), London.

FLOWER, W. H. 1864. Notes on the skeletons of whales in the principal museums of Holland and Belgium, with descriptions of two species apparently new to science. *Proceedings of the Zoological Society of London*, **1864**, 384–420.

FORDYCE, R. E. 1994. *Waipatia maerewhenua*, new genus and new species (Waipatiidae, new family), an archaic Late Oligocene dolphin (Cetacea: Odontoceti: Platanistoidea) from New Zealand. 147–176. *In* BERTA, A. and DEMÉRÉ, T. A. (eds). *Contributions in marine mammal paleontology honoring Frank C. Whitmore, Jr.* Proceedings of the San Diego Society of Natural History, **29**, 268 pp.

—— 2002. Oligocene origins of skim feeding right whales: a small archaic balaenid from New Zealand. *Journal of Vertebrate Paleontology*, **22** (3 Suppl.), 54A.

—— and BARNES, L. G. 1994. The evolutionary history of whales and dolphins. *Annual Review of Earth and Planetary Science*, **22**, 419–455.

—— and DE MUIZON, C. 2001. Evolutionary history of cetaceans: a review. 169–233. *In* MAZIN, J.-M. and DE BUFFRENIL, V. (eds). *Secondary adaptations of tetrapods to life in water*. Verlag Pfeil, München, 367 pp.

FRAAS, E. 1904. Neue Zeuglodonten aus dem unteren Mitteleocän vom Mokattam bei Cairo. *Geologische und Paläontologische Abhandlungen*, **6**, 197–220.

GEISLER, J. H. and LUO, Z. 1996. The petrosal and inner ear of *Herpetocetus* sp. (Mammalia: Cetacea) and their implications for the phylogeny and hearing of archaic mysticetes. *Journal of Paleontology*, **70**, 1045–1066.

—— —— 1998. Relationships of Cetacea to terrestrial Ungulates and the evolution of cranial vasculature in Cete. 163–212. *In* THEWISSEN, J. G. M. (ed.). *The emergence of whales*. Plenum Press, New York, 477 pp.

—— and SANDERS, A. E. 2003. Morphological evidence for the phylogeny of Cetacea. *Journal of Mammalian Evolution*, **10**, 23–129.

——MCGOWEN, M. R., YANG, G. and GATESY, J. 2011. A supermatrix analysis of genomic, morphological, and paleontological data from crown Cetacea. *BMC Evolutionary Biology*, **11**, 112–145.

GRAY, J. E. 1825. Outline of an attempt at the disposition of the Mammalia into tribes and families with a list of the genera apparently appertaining to each tribe. *Philosophical Annals*, **26**, 337–344.

—— 1864. Notes on the Whalebone-Whales; with a synopsis of the species. *The Annals and Magazine of Natural History*, **14**, 345–353.

HUELSENBECK, J. P. 1994. Comparing the stratigraphic record to estimates of phylogeny. *Paleobiology*, **20**, 470–483.

——PETKEWICH, R. M., BISHOP, G. A., BUKRY, D. and ALESHIRE, D. P. 1996. A new Middle Eocene protocetid whale (Mammalia: Cetacea: Archaeoceti) and associated biota from Georgia. *Journal of Paleontology*, **72**, 907–927.

KELLOGG, R. 1924. Description of a new genus and species of whalebone whale from the Calvert Cliffs, Maryland. *Proceedings of the United States National Museum*, **63**, 1–14.

—— 1928. The history of whales – Their adaptation to life in the water. *The Quarterly Review of Biology*, **3**, 29–76, 174–208.

—— 1929. A new cetothere from southern California. *University of California Publications in Geological Sciences*, **18**, 449–457.

—— 1934*a*. The Patagonian fossil whalebone whale *Cetotherium moreni* (Lydekker). *Contributions to Palaeontology, Carnegie Institution, Washington*, **447**, 65–81.

—— 1934*a*. The Patagonian fossil whalebone whale *Cetotherium moreni* (Lydekker). *Contributions to Palaeontology, Carnegie Institution, Washington*, **447**, 65–81.

—— 1934*b*. A new cetothere from the Modelo Formation at Los Angeles, California. *Contributions to Palaeontology, Carnegie Institution, Washington*, **447**, 85–104.

—— (ed.) 1965. Fossil marine mammals from the Miocene Calvert Formation of Maryland and Virginia. *United States National Museum Bulletin*, **247**, 1–45.

—— 1968*a*. Miocene Calvert mysticetes described by Cope. 103–132. *In* KELLOGG, R. (ed.). *Fossil marine mammals from the Miocene Calvert Formation of Maryland and Virginia. United States National Museum Bulletin*, **247**, 103–197.

—— 1968*b*. A hitherto unrecognized Calvert mysticete. 133–161. *In* KELLOGG, R. (ed.). *Fossil marine mammals from the Miocene Calvert Formation of Maryland and Virginia. United States National Museum Bulletin*, **247**, 103–197.

—— 1968*c*. A sharp-nosed cetothere from the Miocene Calvert 163–197. *In* KELLOGG, R. (ed.). *Fossil marine mammals from the Miocene Calvert Formation of Maryland and Virginia. United States National Museum Bulletin*, **247**, 103–197.

—— 1968*d*. Supplement to description of *Parietobalaena palmeri*. 175–197. *In* KELLOGG, R. (ed.). *Fossil marine mammals from the Miocene Calvert Formation of Maryland and Virginia. United States National Museum Bulletin*, **247**, 103–197.

—— 1969. Cetothere skeletons from the Miocene Choptank Formation of Maryland and Virginia. *United States National Museum Bulletin*, **294**, 1–39.

KIMURA, T. 2002. Feeding strategy of an Early Miocene cetothere from the Toyama and Akeyo Formations, central Japan. *Palaeontological Record*, **6**, 179–189.

—— and HASEGAWA, Y. 2010. A new baleen whale (Mysticeti: Cetotheriidae) from the earliest Late Miocene of Japan and a reconsideration of the phylogeny of cetotheres. *Journal of Vertebrate Paleontology*, **30**, 577–591.

—— and OZAWA, T. 2002. A new cetothere (Cetacea: Mysticeti) from the Early Miocene of Japan. *Journal of Vertebrate Paleontology*, **22**, 684–702.

—— SAKAMOTO, O. and HASEGAWA, Y. 1998. A cetothere from the Miocene Chichibumachi Group, Aitama Prefecture, Japan. *Bulletin of the Saitama Museum of Natural History*, **16**, 1–13.

LAMBERT, O. 2005. Phylogenetic affinities of the long-snouted dolphin *Eurhinodelphis* (Cetacea, Odontoceti) from the Miocene of Antwerp. *Palaeontology*, **48**, 653–679.

—— 2008. Sperm whales from the Miocene of the North Sea: a re-appraisal. *Bulletin de l'Institut Royal des Sciences Naturelles de Belgique, Sciences de la Terre*, **78**, 277–316.

—— and LOUWYE, S. 2006. *Archaeoziphius microglenoideus*, a new primitive beaked whale (Mammalia, Cetacea, Odontoceti) from the Middle Miocene of Belgium. *Journal of Vertebrate Paleontology*, **26**, 182–191.

LILLJEBORG, W. 1861. Hvalben, Funna i Jorden par Grayson i Roslagen i Sverige. *Forhandlinger vid et Skandinaviska Naturforskaremotet*, **1860**, 599–616.

LINNAEUS, C. 1758. *Systema Naturae*. Salvii, Holmiae (Stockholm), Sweden, 824 pp.

LOUWYE, S. 2005. The Early and Middle Miocene transgression at the southern border of the North Sea Basin (northern Belgium). *Geological Journal*, **40**, 441–456.

—— DE CONINCK, J. and VERNIERS, J. 2000. Shallow marine Lower and Middle Miocene deposits at the southern margin of the North Sea Basin (northern Belgium): dinoflagellate cyst biostratigraphy and depositional history. *Geological Magazine*, **137**, 381–394.

—— MARQUET, R., BOSSELAERS, M. and LAMBERT, O. 2010. Stratigraphy of an Early-Middle Miocene sequence near Antwerp in northern Belgium (southern North Sea basin). *Geologica Belgica*, **13**, 269–284.

LUO, Z. and GINGERICH, P. D. 1999. Terrestrial Mesonychia to aquatic Cetacea: transformation of the basicranium and evolution of hearing in whales. *University of Michigan, Papers in Paleontology*, **31**, 1–98.

MARX, F. G. 2011. The more the merrier? A large cladistic analysis of mysticetes, and comments on the transition from teeth to baleen. *Journal of Mammalian Evolution*, **18**, 77–100.

MCKENNA, M. C. and BELL, S. K. 1997. *Classification of mammals above the species level*. Columbia University Press, New York, 631 pp.

MCLEOD, S. A., WHITMORE, F. C. Jr and BARNES, L. G. 1993. Evolutionary relationships and classification. 45–70. *In* BURNS, J. J., MONTAGUE, J. J. and COWLES, C. J. (eds). *The Bowhead whale. The Society for Marine Mammalogy, Special Publication*, **2**, 787 pp.

MEAD, J. G. and FORDYCE, R. E. 2009. The therian skull. A lexicon with emphasis on the odontocetes. *Smithsonian Contributions to Zoology*, **627**, 1–248.

MILLER, G. S. 1923. The telescoping of the cetacean skull. *Smithsonian Miscellaneous Collections*, **76**, 1–70.

MITCHELL, E. D. 1989. A new cetacean from the late Eocene La Meseta Formation, Seymour Island, Antarctic Peninsula. *Canadian Journal of Fisheries and Aquatic Sciences*, **46**, 2219–2235.

MORGAN, G. S. 1994. Miocene and Pliocene marine mammal faunas from the Bone Valley Formation of Central Florida. 239–268. *In* BERTA, A. and DEMÉRÉ, T. A. (eds). *Contibutions in marine mammal paleontology honoring Frank C. Whitmore Jr. Proceedings of the San Diego Society of Natural History*, **29**, 268 pp.

NICKEL, R., SCHUMMER, A. and SEIFERLE, E. 1991. *Trattato di anatomia degli animali domestici*, Vol. 1. Edagricole, Bologna, 592 pp.

PACKARD, E. L., KELLOGG, R. and HUBER, E. 1934. Marine mammals. *Contributions to Palaeontology, Carnegie Institution Washington*, **447**, 1–104.

PILLERI, G. 1986. *Beobachtungen an den fossilen Cetaceen des Kaukasus*. Hirnanatomisches Institut Ostermundigen, Vammala, 40 pp.

—— 1989. *Beiträge sur Paläontologie der Cetaceen Perus*. Brain Anatomy Institute, Ostermundigen, Switzerland, 233 pp.

—— and SIBER, H. J. 1989. Neuer Spattertiarer cetotherid (Cetacea, Mysticeti) aus der Pisco Formation Perus. 109–115. *In* PILLERI, G. and SIBER, H. J. (eds). *Beitrage zur Palaontologie der Cetaceen Perus*. Hirnanatomisches Institut Ostermundigen, Vammala, 240 pp.

PORTIS, A. 1885. Catalogo descrittivo dei Talassoterii rinvenuti nei terreni terziari del Piemonte e della Liguria. *Memorie della Reale Accademia delle Scienze di Torino*, **37**, 247–365.

RIEMSLAG, C. 1998. Het zoeken van fossielen aan het strand van Cadzand en de Zwarte polder. 24–28. *In* LINDEMANN, A. (ed). *Geode, Gids voor strandfossielen van Cadzand en Nieuwvliet-Bad*, **30**, 156 pp.

ROTH, F. 1978. *Mesocetus argillarius* sp. n. (Cetacea, Mysticeti) from Upper Miocene of Denmark, with remarks on the lower jaw and the echolocation system in whale phylogeny. *Zoologica Scripta*, **7**, 63–79.

SANDERS, A. E. and BARNES, L. G. 2002*a*. Paleontology of the Late Oligocene Ashley and Chandler Bridge Formations of South Carolina, 2: *Mycromysticetus rothauseni*, a primitive cet-

otheriid mysticete (Mammalia: Cetacea). 271–293. *In* EMRY, R. J. (ed.). *Cenozoic mammals of land and sea: tributes to the career of Clayton E. Ray. Smithsonian Contribution in Paleobiology*, **97**, 372 pp.

—— —— 2002*b*. Paleontology of the late oligocene ashley and chandler bridge formations of South Carolina, 3: Eomysticetidae, a new family of primitive mysticetes (Mammalia: Cetacea). 313–356. *In* EMRY, R. J. (ed.). *Cenozoic mammals of land and sea: tributes to the career of Clayton E. Ray. Smithsonian Contribution to Paleobiology*, **93**, 372 pp.

SCHALLER, O. 1999. *Nomenclatura anatomica veterinaria illustrata*. Delfino Editore, Roma, 637 pp.

SERENO, P. C. 1998. A rationale for phylogenetic definitions, with application to the higher level taxonomy of Dinosauria. *Neues Jahrbuch für Geologie und Paläontologie Abhandlungen*, **210**, 41–83.

—— 1999. Definitions in phylogenetic taxonomy: Critique and rationale. *Systematic Biology*, **48**, 329–351.

SLIJPER, E. J. 1936. Die Cetaceen vergleichend-anatomisch und systematisch. *Capita Zoologica*, **7**, 1–590.

STEEMAN, M. E. 2007. Cladistic analysis and a revised classification of fossil and recent mysticetes. *Zoological Journal of the Linnean Society*, **150**, 875–894.

—— 2009. A new baleen whale from the Late Miocene of Denmark and early mysticete hearing. *Palaeontology*, **52**, 1169–1190.

—— 2010. The extinct baleen whale fauna from the Miocene-Pliocene of Belgium and the diagnostic cetacean ear bones. *Journal of Systematic Paleontology*, **8**, 63–80.

SWOFFORD, D. L. 2002. PAUP – *Phylogenetic Analysis using Parsimony*. Beta Documentation. Laboratory of Molecular Systematics, Smithsonian Institution. Available at: world wide web site http://paup.csit.fsu.edu/.

TRUE, F. W. 1904. The whalebone whales of the western north Atlantic, compared with those occurring in European waters; with some observations on the species of the north Pacific. *Smithsonian Contributions to Knowledge*, **33**, 1–332.

UHEN, M. D. 2010. Paleobiology Database (http://www.paleodb.org/) Online Systematics Archive 9 – Cetacea.

—— FORDYCE, R. E. and BARNES, L. G. 2008. Mysticeti. 607–628. *In* JANIS, C. M., GUNNELL, G. F. and UHEN, M. D. (eds). *Evolution of Tertiary mammals of north America*, Vol. 2. Cambridge University Press, New York, 802 pp.

WHITMORE, F. C. Jr. 1994. Neogene climatic change and the emergence of the modern whale fauna of the North Atlantic ocean. 223–227. *In* BERTA, A. and DEMÉRÉ, T. A. (eds). *Contributions in marine mammal paleontology honoring Frank C. Whitmore Jr. Proceedings of the San Diego Society of Natural History*, **29**, 268 pp.

—— and BARNES, L. G. 2008. The Herpetocetinae, a new subfamily of extinct baleen whales (Mammalia, Cetacea, Cetotheriidae. 141–180. *In* RAY, C. E., BOHASKA, D. J., KORETSKY, I. A., WARD, L. W. and BARNES, L. G. (eds). *Geology and paleontology of the Lee Creek Mine, North Carolina, IV. Virginia Museum of Natural History Special Publication*, **14**, 516 pp.

ZBYSZEWSKI, G. 1953. Note sur une mandibule *d'Isocetus* trouvée à Mutela. *Boletim da Sociedade Geológica de Portugal*, **11**, 91–92.